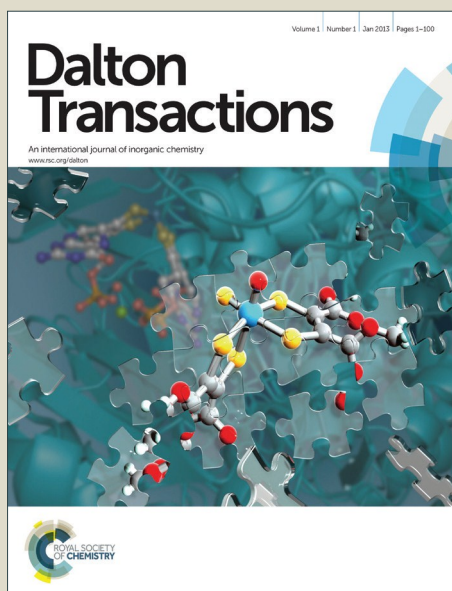


# Dalton Transactions

Accepted Manuscript



This article can be cited before page numbers have been issued, to do this please use: M. Balamurugan, S. Eringathodi and M. Palaniandavar, *Dalton Trans.*, 2016, DOI: 10.1039/C6DT01059H.



This is an *Accepted Manuscript*, which has been through the Royal Society of Chemistry peer review process and has been accepted for publication.

*Accepted Manuscripts* are published online shortly after acceptance, before technical editing, formatting and proof reading. Using this free service, authors can make their results available to the community, in citable form, before we publish the edited article. We will replace this *Accepted Manuscript* with the edited and formatted *Advance Article* as soon as it is available.

You can find more information about *Accepted Manuscripts* in the [Information for Authors](#).

Please note that technical editing may introduce minor changes to the text and/or graphics, which may alter content. The journal's standard [Terms & Conditions](#) and the [Ethical guidelines](#) still apply. In no event shall the Royal Society of Chemistry be held responsible for any errors or omissions in this *Accepted Manuscript* or any consequences arising from the use of any information it contains.

Communicated to: Dalton Trans.  
Ms Type : Article

## $\mu$ -Oxo- and Bis( $\mu$ -carboxylato)-bridged Diiron(III) Complexes of a 3N Ligand as Catalysts for Alkane Hydroxylation: Stereoelectronic Factors of Carboxylate Bridge Determine the Catalytic Efficiency

Mani Balamurugan,<sup>a</sup> Eringathodi Suresh,<sup>b</sup> and Mallayan Palaniandavar<sup>a\*</sup>

<sup>a</sup>*School of Chemistry, Bharathidasan University, Tiruchirappalli - 620024, Tamil Nadu, India.*

<sup>b</sup>*Analytical Science Discipline, Central Salt and Marine Chemicals Research Institute, Bhavnagar - 364 002, India.*

---

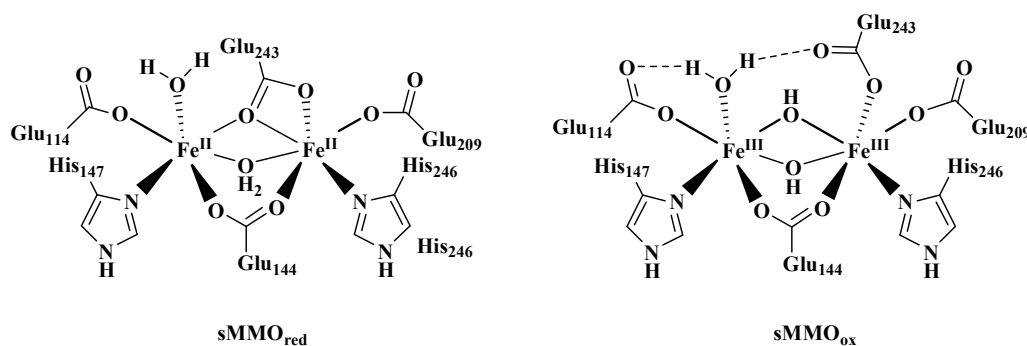
\*To whom correspondence should be addressed, e-mail: [palanim51@yahoo.com](mailto:palanim51@yahoo.com) and [palaniandavarm@gmail.com](mailto:palaniandavarm@gmail.com)

## Abstract

A series of non-heme ( $\mu$ -oxo)bis( $\mu$ -dicarboxylato)-bridged diiron(III) complexes  $[\text{Fe}_2(\text{O})(\text{OOCH})_2(\text{L})_2]^{2+}$  **1**,  $[\text{Fe}_2(\text{O})(\text{OAc})_2(\text{L})_2]^{2+}$  **2**,  $[\text{Fe}_2(\text{O})(\text{Me}_3\text{AcO})_2(\text{L})_2]^{2+}$  **3**,  $[\text{Fe}_2(\text{O})(\text{OBz})_2(\text{L})_2]^{2+}$  **4**,  $[\text{Fe}_2(\text{O})(\text{Ph}_2\text{AcO})_2(\text{L})_2]^{2+}$  **5** and  $[\text{Fe}_2(\text{O})(\text{Ph}_3\text{AcO})_3(\text{L})_2]^{2+}$  **6**, where L = *N,N*-dimethyl-*N'*-(pyrid-2-ylmethyl)ethylenediamine,  $\text{OAc}^-$  = acetate,  $\text{Me}_3\text{AcO}^-$  = trimethylacetate,  $\text{OBz}^-$  = benzoate,  $\text{Ph}_2\text{AcO}^-$  = diphenylacetate and  $\text{Ph}_3\text{AcO}^-$  = triphenylacetate, have been isolated and characterized using elemental analysis and spectral and electrochemical techniques. They have been studied as catalysts for selective oxidation of alkanes using *m*-chloroperbenzoic acid (*m*-CPBA) as the oxidant. The complexes **2**, **3**, and **4** possess a distorted bioctahedral geometry in which each iron atom is coordinated to the oxygen atom of the  $\mu$ -oxo bridge, two oxygen atoms of the  $\mu$ -carboxylate bridge and three nitrogen atoms of the 3N ligand. In acetonitrile/dichloromethane solvent mixture all the complexes display a d-d band characteristic of triply bridged diiron(III) core revealing that they retain their identity in solution. Upon replacing electron-donating substituent on the bridging carboxylates by electron-withdrawing one the  $E_{1/2}$  value of the one-electron  $\text{Fe}^{\text{III}}\text{Fe}^{\text{III}} \rightarrow \text{Fe}^{\text{III}}\text{Fe}^{\text{II}}$  reduction becomes less negative. On adding one equivalent of  $\text{Et}_3\text{N}$  to a mixture of one equivalent of the complex and excess of *m*-CPBA in acetonitrile/dichloromethane solvent mixture an intense absorption band ( $\lambda_{\text{max}}$ , 680-720 nm) appears, which corresponds to the formation of a mixture of complex species. All the complexes act as efficient catalysts for hydroxylation of cyclohexane with 380 - 500 total turnover numbers and good alcohol selectivity (A/K, 6.0-10.1). Adamantane is selectively oxidized to 1-adamantanol and 2-adamantanol (3°/2°, 12.9-17.1) along with small amount of 2-adamantanone (Total TON, 381-476), and interestingly, the sterically demanding trimethylacetate bridge around the diiron(III) centre leads to high 3°/2° bond selectivity; on the other hand, sterically demanding triphenylacetate bridge gives lower 3°/2° bond selectivity. A remarkable linear correlation between the  $pK_a$  of the bridging carboxylate and TON for both cyclohexane and adamantane oxidation is observed illustrating the highest catalytic activity for **3** with strongly electron-releasing trimethylacetate bridges.

## Introduction

In nature iron containing enzymes like methane monooxygenases, cytochrome P450 and bleomycin play a vital role in catalyzing many biologically essential organic transformations. Particularly, the soluble methane monooxygenases (sMMO), which catalyze the oxidation of methane to methanol using dioxygen, are the widely investigated metalloenzymes.<sup>1-10</sup> Also, selective hydroxylation of hydrocarbons under mild conditions is a challenging scientific goal in synthetic organic chemistry,<sup>11</sup> because industrial hydroxylation processes typically involve high temperatures and high pressures, while enzymes catalyze these reactions under mild reaction conditions and follow different methodologies from those of industrial processes. Thus the active site of the reduced form of sMMO possesses a diiron(II) center containing four glutamate and two histidine residues, and the iron atoms are bridged by two carboxylate ligands from glutamate residues. On the other hand, the oxidized form contains only one carboxylate and two hydroxo bridges (sMMO<sub>ox</sub>, Scheme 1) in its active site.<sup>12</sup> The interesting fact that several non-heme diiron proteins such as ribonucleotide reductases (RNR)<sup>13</sup> and hemerythrin (Hr)<sup>14</sup> also contain at least two carboxylate bridges in the active site of their reduced forms, but they are different in their functions. Interestingly, the bridging units also play a vital role in dictating the function of the enzymes. So, the isolation and study of synthetic models containing the structural core  $[\text{Fe}_2(\text{O})(\text{O}_2\text{CR})_2]^{2+}$  have received greater attention among the bioinorganic communities.<sup>15-17</sup> Also, a wide variety of coordination environments and bridging modes around the iron center in non-heme enzymes generate distinct oxidizing intermediates, which are supposed to result in their intrinsic catalytic transformations.<sup>18,19</sup> Inspired by these enzymes efforts have been made during the last two decades to develop synthetic models for sMMO and study the mechanism of  $\text{O}_2$  activation involved in the oxygenation of alkanes.<sup>9,20</sup> The study of synthetic diiron

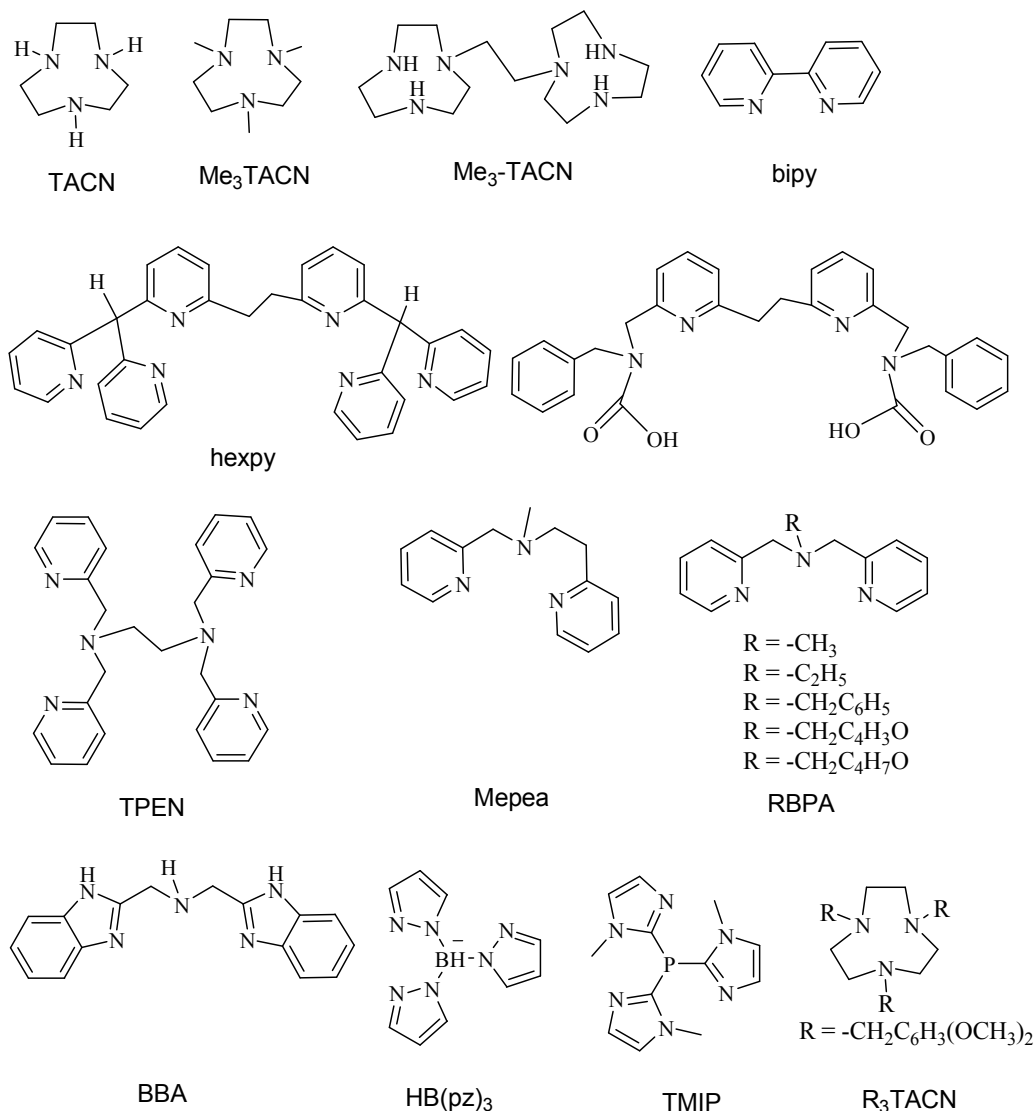


**Scheme 1:** Active site structures of soluble methane monooxygenase

compounds with different carboxylate motifs has mainly served as benchmarks for illustrating the oxidizing intermediates and catalytic pathway of the enzymes, and efforts to make use of them as functional mimics are scarce.

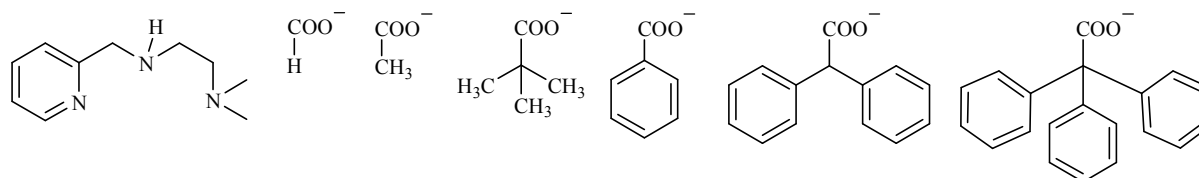
Many synthetic models have been isolated and studied as structural and functional models for metHr and sMMO containing the structural motif  $[\text{Fe}_2(\text{O})(\text{O}_2\text{CR})_2(\text{L})_2]^{2+}$ , where L is a tridentate 3N ligand.<sup>21–25</sup> Christou *et al.* have isolated triply-bridged diiron(III) complexes<sup>26,27</sup> derived from bipyridine and used them as catalysts for alkane hydroxylation using *tert*-butylhydroperoxide (*t*-BuOOH) as oxidant. Kitajima *et al.* studied the triply-bridged diiron(III) complex<sup>28</sup>  $[\text{Fe}_2(\text{O})(\text{O}_2\text{CCH}_3)_2(\text{HB}(\text{pz})_3)]^{2+}$  as catalyst for alkane hydroxylation using molecular oxygen (in the presence of an electron source), but low selectivity and poor yields were observed for these reactions. Later, Kodera *et al.* have isolated the complex  $[\text{Fe}_2(\text{O})(\text{O}_2\text{CCH}_3)_2(\text{hexpy})](\text{ClO}_4)_2$ , which catalyses the oxidation of cyclohexane with notable alcohol/ketone ratio (A/K, 2.4) and that of adamantane with moderate tertiary/secondary carbon ratio ( $3^\circ/2^\circ$ , 4.2) using *m*-chloroperbenzoic acid (*m*-CPBA) as oxidant.<sup>29–31</sup> Recently, Itoh *et al.*<sup>32</sup> have isolated the triply-bridged diiron(III) complex  $[\text{Fe}_2(\text{O})(\text{O}_2\text{CCH}_3)_2(\text{L})](\text{ClO}_4)_2$ , where L is 1,2-bis(*N*-benzyl-2-aminomethyl-6-pyridyl)ethane-*N',N'*-diacetic acid, which catalyses hydroxylation of cyclohexane (A/K, 10.0) and adamantane ( $3^\circ/2^\circ$ , 13.6) with selectivity using hydrogen peroxide. We have also recently reported<sup>33</sup> triply-bridged diiron(III) complexes of the type  $[\text{Fe}_2\text{O}(\textit{i}$ Bu-bpa/Bz-bpa)<sub>2</sub>(RCOO)<sub>2</sub>]<sup>2+</sup>, where *i*Bu-bpa = *N,N*-bis(pyrid-2-ylmethyl)-*iso*-butylamine, Bz-bpa = *N,N*-bis(pyrid-2-ylmethyl)benzylamine (Scheme 2), R = -CH<sub>3</sub>, -C<sub>6</sub>H<sub>5</sub>, which act as efficient catalysts (A/K, 10.2–13.8) towards alkane hydroxylation.<sup>33</sup> Also, many oxo-bridged diiron(III) complexes of tetradentate ligands have been isolated<sup>34–40</sup> as synthetic models for the diiron(III) biosites, but the catalytic efficiency and selectivity of these systems are lower than those of the enzymes. However, the basis for the high selectivity, efficiency and the mechanistic pathway of alkane hydroxylation reaction catalyzed by small molecule analogues remains unclear.

All the above observations encouraged us to isolate diiron(III) complexes of tridentate (3N) ligands with various carboxylate bridging ligands, such as  $[\text{Fe}_2(\text{O})(\text{OOCH})_2(\text{L})_2](\text{ClO}_4)_2$  **1**,  $[\text{Fe}_2(\text{O})(\text{OAc})_2(\text{L})_2](\text{ClO}_4)_2$  **2**,  $[\text{Fe}_2(\text{O})(\text{Me}_3\text{Ac})_2(\text{L})_2](\text{ClO}_4)_2$  **3**,  $[\text{Fe}_2(\text{O})(\text{OBz})_2(\text{L})_2](\text{ClO}_4)_2$  **4**,  $[\text{Fe}_2(\text{O})(\text{Ph}_2\text{Ac})_2(\text{L})_2](\text{ClO}_4)_2$  **5** and  $[\text{Fe}_2(\text{O})(\text{Ph}_3\text{Ac})_3(\text{L})_2](\text{ClO}_4)_2$  **6**, where L = *N,N*-dimethyl-*N'*-(pyrid-2-ylmethyl)ethylenediamine (Scheme 3), and study their use as functional models for the



**Scheme 2.** Structures of bi- and tridentate 3N ligands of diiron(III) complexes reported already

alkane hydroxylation reactions catalyzed by sMMO. We intend to study the steric and electronic effects of different carboxylate bridges on the highly selective hydroxylation of alkanes. The 3N



**Scheme 3.** Structures of tridentate 3N and bridging carboxylate ligands employed in the study

nitrogen donors in the enzymes and the weakly coordinating  $-NMe_2$  donor is expected<sup>51</sup> to enhance the Lewis acidity of the diiron(III) core and hence the coordinating ability of the carboxylate bridges. The single-crystal X-ray structures of **2**, **3** and **4** have been determined to show that each iron atom in the complexes is coordinated to one oxygen atom of the  $\mu$ -oxo bridge and two oxygen atoms of both the  $\mu$ -carboxylate bridges apart from three nitrogen atoms of the 3N ligand. We have observed that all the six complexes show efficient hydroxylation of cyclohexane and adamantane with approximately 380-500 turn over numbers and good selectivity (A/K ratio, 6.0-10.1;  $3^\circ/2^\circ$ , 12.9-17.1), as tuned, interestingly, by the varying electron-donating and electron-withdrawing nature of substituents on the carboxylate bridging ligands.

## Experimental

### Materials

Pyridine-2-carboxaldehyde, *N,N*-dimethylethylenediamine, iron(III) perchlorate hydrate, adamantane, cumene, trimethylacetic acid, diphenylacetic acid, triphenylacetic acid, *m*-chloroperbenzoic acid, sodium borohydride, tetra-*N*-butylammonium bromide (Aldrich), triethylamine, benzoic acid, acetic acid glacial, formic acid (Merck, India), cyclohexane (Ranbaxy) and ethanol (Hayman Limited, England) were used as received. Dichloromethane, diethylether, tetrahydrofuran, acetonitrile (Merck, India) and methanol (Sisco Research Laboratory, Mumbai) were distilled before use. The supporting electrolyte tetra-*N*-butylammonium perchlorate (TBAP) was prepared in water and recrystallized twice from aqueous ethanol. The ligand *N,N*-dimethyl-*N'*-(pyrid-2-ylmethyl)ethane-1,2-diamine was prepared as reported<sup>41</sup> earlier.

### Synthesis of Complexes

The general procedure involves the addition of carboxylic acids (2.0 mmol) previously neutralized with 2.0 mmol of triethylamine/sodium hydroxide to a mixture of 924 mg of  $Fe(ClO_4)_3 \cdot 6H_2O$  (2.0 mmol) in methanol (5 mL) containing  $H_2O$  (0.1 mL) and stirred for 30 min at room temperature. To this, a methanol (8 mL) solution of the ligand (2.0 mmol) was added and the resulting dark red solution was turned reddish brown or green upon stirring for an hour. Reddish brown or green precipitate or microcrystals of diiron(III) complexes were formed within

24 hr upon standing. The precipitates were collected by suction filtration, washed with small quantities of cold methanol and dried *in vacuo*.

**[Fe<sub>2</sub>(O)(O<sub>2</sub>CH)<sub>2</sub>(L)<sub>2</sub>](ClO<sub>4</sub>)<sub>2</sub> (1).** Yield: 0.56 g (72%). ESI-MS, *m/z* = 677.0 [(M–ClO<sub>4</sub>)<sup>+</sup>]; 289.0 [(M–2ClO<sub>4</sub>)<sup>2+</sup>]. Anal. Calcd. for C<sub>22</sub>H<sub>38</sub>Cl<sub>2</sub>Fe<sub>2</sub>N<sub>6</sub>O<sub>13</sub>: C 34.00, H 4.93, N 10.81. Found C 34.04, H 4.90, N 10.75.

**[Fe<sub>2</sub>(O)(OAc)<sub>2</sub>(L)<sub>2</sub>](ClO<sub>4</sub>)<sub>2</sub> (2).** Yield: 0.69 g (86%). ESI-MS, *m/z* = 705.0 [(M–ClO<sub>4</sub>)<sup>+</sup>]; 303.0 [(M–2ClO<sub>4</sub>)<sup>2+</sup>]. Anal. Calcd. for C<sub>24</sub>H<sub>42</sub>Fe<sub>2</sub>N<sub>6</sub>O<sub>13</sub>Cl<sub>2</sub>: C 35.80, H 5.26, N 10.44. Found C 35.79, H 5.28, N 10.39. Single crystals of **2** suitable for X-ray diffraction were obtained by the slow evaporation of methanol/acetonitrile solution of the complex.

**[Fe<sub>2</sub>(O)(Me<sub>3</sub>AcO)<sub>2</sub>(L)<sub>2</sub>](ClO<sub>4</sub>)<sub>2</sub>·CH<sub>3</sub>CN (3).** Yield: 0.72 g (77%). ESI-MS, *m/z* = 787.1 [(M–ClO<sub>4</sub>–CH<sub>3</sub>CN)<sup>+</sup>]; 344.1 [(M–2ClO<sub>4</sub>–CH<sub>3</sub>CN)<sup>2+</sup>]. Anal. Calcd. for C<sub>32</sub>H<sub>55</sub>Fe<sub>2</sub>N<sub>7</sub>O<sub>13</sub>Cl<sub>2</sub>: C 41.40, H 5.97, N 10.56. Found C 41.42, H 5.95, N 10.50. Single crystals of **3** suitable for X-ray diffraction were obtained by the slow evaporation of methanol/acetonitrile solution of the complex.

**[Fe<sub>2</sub>(O)(OBz)<sub>2</sub>(L)<sub>2</sub>](ClO<sub>4</sub>)<sub>2</sub>·CH<sub>3</sub>OH·H<sub>2</sub>O (4).** Yield: 0.79 g (81%). ESI-MS, *m/z* = 827.0 [(M–ClO<sub>4</sub>–CH<sub>3</sub>OH–H<sub>2</sub>O)<sup>+</sup>]; 364.2 [(M–2ClO<sub>4</sub>–CH<sub>3</sub>OH–H<sub>2</sub>O)<sup>2+</sup>]. Anal. Calcd. for C<sub>35</sub>H<sub>50</sub>Fe<sub>2</sub>N<sub>6</sub>O<sub>15</sub>Cl<sub>2</sub>: C 43.01, H 5.16, N 8.60. Found C 43.09, H 5.12, N 8.55. Single crystals of **4** suitable for X-ray diffraction were obtained by slow evaporation of methanol/acetonitrile solution of the complex.

**[Fe<sub>2</sub>(O)(Ph<sub>2</sub>AcO)<sub>2</sub>(L)<sub>2</sub>](ClO<sub>4</sub>)<sub>2</sub> (5).** Yield: 0.84 g (76%). ESI-MS, *m/z* = 1007.2 [(M–ClO<sub>4</sub>)<sup>+</sup>]; 454.1 [(M–2ClO<sub>4</sub>)<sup>2+</sup>]. Anal. Calcd. for C<sub>48</sub>H<sub>56</sub>Cl<sub>2</sub>Fe<sub>2</sub>N<sub>6</sub>O<sub>13</sub>: C 52.05, H 5.10, N 7.59. Found C 52.09, H 5.17, N 7.58.

**[Fe<sub>2</sub>(O)(Ph<sub>3</sub>AcO)<sub>2</sub>(L)<sub>2</sub>](ClO<sub>4</sub>)<sub>2</sub> (6).** Yield: 0.88 g (70%). ESI-MS, *m/z* = 1159.2 [(M–ClO<sub>4</sub>)<sup>+</sup>]; 530.1 [(M–2ClO<sub>4</sub>)<sup>2+</sup>]. Anal. Calcd. for C<sub>60</sub>H<sub>64</sub>Cl<sub>2</sub>Fe<sub>2</sub>N<sub>6</sub>O<sub>13</sub>: C 57.20, H 5.12, N 6.67. Found C 57.23, H 5.15, N 6.69.

**Caution:** Perchlorate salts of the compounds are potentially explosive! Only small quantities of these compounds should be prepared and suitable precautions should be taken when they are handled.

## Catalytic Oxidations

The oxidation of alkanes was carried out at room temperature under an atmosphere of air. In a typical reaction, the oxidant *m*-CPBA ( $0.8 \text{ mol dm}^{-3}$ ) was added to a mixture of diiron(III) complex ( $1 \times 10^{-3} \text{ mmol dm}^{-3}$ ) and alkanes ( $3 \text{ mol dm}^{-3}$ ) in  $\text{CH}_2\text{Cl}_2:\text{CH}_3\text{CN}$  mixture (4:1 v/v). After 30 min (Figure S5) the reaction was quenched with triphenylphosphine, the reaction mixture was filtered over a silica column and then eluted with diethylether. An internal standard (bromobenzene) was added at this point and the solution was subjected to GC analysis. The mixture of organic products were identified by GC-MS and quantitatively analyzed by HP 6890 series GC equipped with HP-5 capillary column ( $30 \text{ m} \times 0.32 \text{ mm} \times 2.5 \mu\text{m}$ ) using a calibration curve obtained with authentic compounds. All of the products were quantified using GC (FID) with the following temperature program: injector temperature  $130 \text{ }^\circ\text{C}$ ; initial temperature  $60 \text{ }^\circ\text{C}$ , heating rate  $10 \text{ to } 130 \text{ }^\circ\text{C min}^{-1}$ , increasing the temperature to  $160 \text{ }^\circ\text{C}$  at a rate of  $2 \text{ }^\circ\text{C min}^{-1}$ , and then increasing the temperature to  $260 \text{ }^\circ\text{C}$  at a rate of  $5 \text{ }^\circ\text{C min}^{-1}$ ; FID temperature  $280 \text{ }^\circ\text{C}$ . GC-MS analysis was performed under conditions identical to those used for GC analysis. The averages of three measurements are reported.

## Physical Measurements

Elemental analyses were performed on a Perkin Elmer Series II CHNS/O Analyzer 2400.  $^1\text{H}$  NMR spectra were recorded on a Bruker 400 MHz NMR spectrometer. Electronic spectra were recorded on an Agilent 8453 Diode Array Spectrophotometer. Low temperature spectra were obtained on an Agilent 8453 Diode Array Spectrophotometer equipped with an UNISOKU USP-203 cryostat. Electrospray-ionization mass-spectrum (ESI-MS) analyses were recorded on a Micromass Quattro II triple quadrupole mass spectrometer. Cyclic voltammetry (CV) and differential pulse voltammetry (DPV) were performed at  $25 \pm 0.2 \text{ }^\circ\text{C}$  using a three-electrode cell configuration. A platinum sphere, a platinum plate and  $\text{Ag(s)}/\text{AgNO}_3$  were used as working, auxiliary and reference electrodes, respectively. The platinum sphere electrode was sonicated for two minutes in dilute nitric acid, dilute hydrazine hydrate and in double distilled water to remove the impurities. The reference electrode for non-aqueous solution was  $\text{Ag(s)}/\text{Ag}^+$ , which consists of a Ag wire immersed in a solution of  $\text{AgNO}_3$  ( $0.01 \text{ M}$ ) and *tetra-N*-butylammonium perchlorate ( $0.1 \text{ M}$ ) in acetonitrile placed in a tube fitted with a vycor plug. The instruments utilized included an EG & G PAR 273 Potentiostat/Galvanostat and P-IV computer along with

EG & G M270 software to carry out the experiments and to acquire the data. The temperature of the electrochemical cell was maintained by a cryo-circulator (HAAKE D8-G). The  $E_{1/2}$  values observed under identical conditions for Fc/Fc<sup>+</sup> couple in acetonitrile was 0.102 V with respect to Ag/Ag<sup>+</sup> reference electrode. The experimental solutions were deoxygenated by bubbling research grade nitrogen and an atmosphere of nitrogen was maintained over the solution during measurements. The products were analyzed by using Hewlett Packard (HP) 6890 GC series Gas Chromatograph equipped with a FID detector and a HP-5 capillary column (30 m × 0.32 mm × 2.5 μm). GC-MS analysis was performed on an Agilent GC-MS equipped with 7890A GC series (HP-5 capillary column) and 5975C inert MSD under conditions that are identical to that used for GC analysis.

### Crystallographic Data Collection and Structure Refinement

The diffraction experiments were carried out on a Bruker SMART APEX diffractometer equipped with a CCD area detector. High quality crystals, suitable for X-ray diffraction was chosen after careful examination under an optical microscope. Intensity data for the crystals were collected using MoK $\alpha$  ( $\lambda = 0.71073 \text{ \AA}$ ) radiation on a Bruker SMART APEX diffractometer equipped with a CCD area detector at 100 and 293 K. The structure was solved by direct methods using the SHELXS-97 and OLEX 2.<sup>42</sup> The refinement and all further calculations were carried out using SHELXL-97.<sup>42</sup> The SMART<sup>43</sup> program was used for collecting frames of data, indexing reflection and determination of lattice parameters; SAINT<sup>44</sup> program for integration of the intensity of reflections and scaling; SADABS<sup>45a</sup> program for absorption correction, and the SHELXTL<sup>42</sup> program for space group and structure determination, and least-squares refinements on  $F^2$ . The disordered solvent molecule present in the lattice of **4** is removed by SQUEEZ function in PLATON.<sup>45b,c</sup> The structure was solved by heavy atom method and other non-hydrogen atoms were located in successive difference Fourier syntheses. Crystal data and additional details of the data collection and refinement of the structure are presented in Table 1. The selected bond lengths and bond angles are listed in Table 2.

### Results and Discussion

**Synthesis and characterization of 3N ligand and diiron(III) complexes.** The tridentate 3N ligand was synthesized according to known procedures, which involve Schiff base condensation

of *N,N*-dimethylethylenediamine with pyridine-2-carboxaldehyde followed by reduction with NaBH<sub>4</sub> and characterized by <sup>1</sup>H NMR and mass spectrometry.<sup>41</sup> The diiron(III) complexes **1** – **6** were prepared by adding one equivalent of the 3N ligand to an aqueous methanol solution containing one equivalent each of Fe(ClO<sub>4</sub>)<sub>3</sub>·6H<sub>2</sub>O, the carboxylic acid and triethylamine. All of them are formulated as [Fe<sub>2</sub>(O)(O<sub>2</sub>CR)<sub>2</sub>(L)<sub>2</sub>](ClO<sub>4</sub>)<sub>2</sub> on the basis of elemental analysis, UV-Vis spectroscopy, ESI-MS and X-ray crystal structures of **2**, **3** and **4**. All the complexes with different bridging carboxylate groups are expected to mimic the active site environment of the substrate-bound enzyme sMMO and have been chosen to model the alkane hydroxylation reactions of the enzyme.

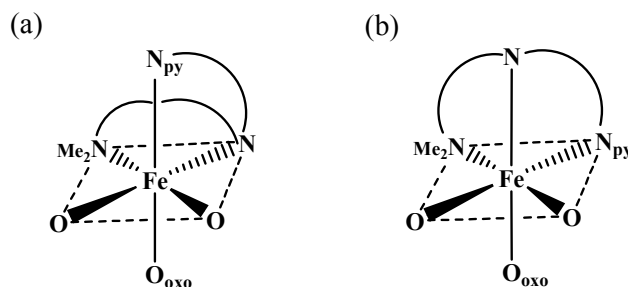
### Description of X-ray Crystal Structures of [Fe<sub>2</sub>(O)(OAc)<sub>2</sub>(L)<sub>2</sub>](ClO<sub>4</sub>)<sub>2</sub> **2**, [Fe<sub>2</sub>(O)(Me<sub>3</sub>AcO)<sub>2</sub>(L)<sub>2</sub>](ClO<sub>4</sub>)<sub>2</sub> **3** and [Fe<sub>2</sub>(O)(OBz)<sub>2</sub>(L)<sub>2</sub>](ClO<sub>4</sub>)<sub>2</sub> **4**

The molecular structure of the dimeric cation of [Fe<sub>2</sub>(O)(OAc)<sub>2</sub>(L)<sub>2</sub>]<sup>2+</sup> **2** is shown in Figure 1 together with the atom numbering scheme and the selected bond lengths and bond angles are collected in Table 2. The molecule contains an inversion centre and the coordination geometry around each iron atom in the diiron(III) complex **2** is distorted octahedral constituted by the oxygen atom of the μ-oxo bridge, two oxygen atoms one each from the μ-acetate bridges and three amine nitrogen atoms of the 3N ligand. The coordination geometry of the complex cation is very similar to those of complexes<sup>23,40,46-50</sup> with (μ-oxo)bis(μ-carboxylato)diiron(III) core structures. The tridentate ligand capping the two ends of the (μ-oxo)bis(μ-carboxylato)-diiron(III) cluster coordinates to iron(III) in a least strained facial rather than meridional fashion (Scheme 4). The Fe-N<sub>py</sub> (2.202 Å) and Fe-N<sub>amine</sub> (2.170(3), 2.234(3) Å) bond distances fall respectively in the ranges 2.100(10) - 2.227(4) Å and 2.160(5) - 2.334(7) Å observed for mono-<sup>51</sup> and diiron(III)<sup>25,30,40,52,53</sup> complexes reported in the literature. The Fe-N<sub>amine</sub> bond (2.234(3) Å) formed by the terminal amine nitrogen of the tridentate ligand is longer than the Fe-N<sub>py</sub> bond (2.202(2) Å) obviously due to sp<sup>3</sup> and sp<sup>2</sup> hybridizations respectively of the tertiary amine and pyridyl nitrogen atoms. However, the Fe-N<sub>py</sub> bond is longer (cf. below, **3**) than the Fe-N<sub>amine</sub> bond (2.170(3) Å) involving sp<sup>3</sup> hybridized central amine nitrogen due to the trans effect exerted by the strongly coordinated μ-oxo bridge. Also, the terminal Fe-N<sub>amine</sub> bond is longer than the central Fe-N<sub>amine</sub> bond, which is expected. The Fe-O<sub>acetate</sub> bond distances (1.988(2), 2.069(2) Å)

fall within the range 1.98 - 2.142 Å observed for similar ( $\mu$ -oxo)bis( $\mu$ -carboxylato)diiron(III) complexes.<sup>29-40,54</sup>

The X-ray crystal structure of the dimeric cation of  $[\text{Fe}_2(\text{O})(\text{Me}_3\text{AcO})_2(\text{L})_2]^{2+}$  **3** is shown in Figure 2 together with the atom numbering scheme and the selected bond lengths and bond angles are collected in Table 2. The coordination geometry of **3** is similar to that of **2** but no inversion centre is present. Each iron(III) centre possesses a distorted octahedral coordination geometry with small differences in bond lengths and bond angles of the other centre. The Fe-N<sub>py</sub> bond in **3** (2.145(3), 2.159(3) Å) is shorter than the Fe-N<sub>amine</sub> bonds formed by the central (2.192(3), 2.181(3) Å) and terminal (2.216(3), 2.225(3) Å) tertiary amine nitrogen atoms, which is expected of the sp<sup>2</sup> and sp<sup>3</sup> hybridizations respectively of the pyridyl and tertiary amine nitrogen atoms. Also, the Fe-N<sub>amine</sub> bond formed by the terminal amine nitrogen atom is longer than the central amine nitrogen, as expected. Interestingly, the Fe-N<sub>py</sub> bond in **2** is much longer than that in **3** confirming the trans effect of  $\mu$ -oxo bond in the former. The presence of electron-releasing methyl groups in **3** is expected to render the coordination of trimethylacetate anion stronger (cf. below) than that of acetate anion in **2**. However, the Fe-O<sub>carboxylate</sub> bond distances in **3** (2.021 - 2.069 Å) are longer than those (1.988, 2.069 Å) in **2**. So it is evident that the steric bulk rather than electronic effect of trimethylacetate anion is important.

The X-ray crystal structure of the dimeric cation of  $[\text{Fe}_2(\text{O})(\text{OBz})_2(\text{L})_2]^{2+}$  **4** is shown in Figure 3 together with the atom numbering scheme and the selected bond lengths and bond angles are collected in Table 2. The coordination geometry of **4** is similar to that of **3** and each iron(III) center possesses a distorted octahedral coordination geometry with small differences in bond lengths and bond angles. As for **3**, the Fe-N<sub>py</sub> bonds in **4** (2.148(4), 2.158(5) Å) are shorter than the Fe-N<sub>amine</sub> bonds formed by the central (2.219(4), 2.198(5) Å) and terminal (2.203(4), 2.192(4) Å) tertiary amine nitrogen atoms, as expected. Interestingly, the Fe-N<sub>amine</sub> bond formed



**Scheme 4.** Mode of coordination of 3N ligand with change in **2** (a) and **3** and **4** (b)

by the central amine nitrogen atom in **4**, unlike in **3**, is longer than the Fe-N<sub>amine</sub> bonds formed by the terminal amine nitrogen atom. The replacement of the acetate anion in **2** by the electron-withdrawing benzoate anion as in **4** renders one of the Fe-O<sub>carboxylate</sub> bonds weaker (2.001 – 2.057 Å), causing the terminal Fe-N<sub>amine</sub> and Fe-N<sub>py</sub> bonds to become stronger by trans effect and consequently, the Fe-N<sub>amine</sub> bond formed by the central amine nitrogen becomes longer. Similar trends in bond lengths have been observed on replacing the acetate bridges in [Fe<sub>2</sub>(O)(OAc)<sub>2</sub>(mbpa)<sub>2</sub>]<sup>2+</sup>,<sup>55a</sup> where mbpa is *N,N*-bis(pyrid-2-ylmethyl)methylamine, by benzoate bridges to give [Fe<sub>2</sub>(O)(OBz)<sub>2</sub>(mbpa)<sub>2</sub>]<sup>2+</sup>.<sup>55b</sup>

Interestingly, the central amine nitrogen atom of the capping ligand in **3** and **4** is axial to Fe(1)O(2)O(3)N(1)N(3) plane and is coordinated trans to the μ-oxo bridge (Scheme 4), which is in sharp contrast to the terminal pyridyl nitrogen in **2** located trans to the μ-oxo bridge. Upon replacing the acetate bridges in **2** by trimethylacetate (**3**) or benzoate (**4**) bridge the coordination mode of 3N ligand changes and is similar to that found in the analogous 3N ligand complexes [Fe<sub>2</sub>(O)(OAc/OBz)<sub>2</sub>(mbpa)<sub>2</sub>]<sup>2+</sup>,<sup>55</sup> and [Fe<sub>2</sub>(O)(OBz)<sub>2</sub>(bba)<sub>2</sub>]<sup>2+</sup>,<sup>56</sup> where bba is bis(benzimidazol-2-ylmethyl)amine. A weaker coordination of the bridging carboxylate, caused by steric or electron-withdrawing effect, requires a stronger Fe-N bond, which is fulfilled by the more strongly coordinating pyridine rather than weakly coordinating amine nitrogen atom, leading to the observed change in mode of coordination of capping ligand.

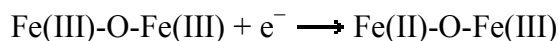
The Fe–O<sub>oxo</sub> bond distance in **2** (Fe(1)–O(1), 1.791(2) Å), **3** (1.796(2), 1.792 (2) Å) and **4** (1.788(3), 1.794(3) Å) falls within the range 1.73–1.82 Å found for oxo-bridged diiron(III) complexes reported<sup>23,40,46-50</sup> in the literature and for [Fe<sub>2</sub>OC<sub>l</sub>]<sub>6</sub><sup>2-</sup>.<sup>57-59</sup> The Fe–O–Fe bond angle (**2**, 120.27(16); **3**, 116.96(11); **4**, 119.32(16)°) is very close to those observed for the analogous complexes [Fe<sub>2</sub>(O)(OAc/OBz)<sub>2</sub>(mbpa)<sub>2</sub>]<sup>2+</sup>,<sup>55</sup> and is well outside the range for the singly-<sup>60</sup> and doubly-bridged<sup>61</sup> complexes (140–180°). The Fe---Fe separation (**2**, 3.107; **3**, 3.059; **4**, 3.091 Å) is shorter than those in singly- and doubly-bridged μ-oxo-diiron(III) complexes (3.4–3.6 Å), which is expected of the presence of three ligand bridges. The Fe---Fe separation in **2** (3.107 Å) is slightly longer than those in **3** (3.059 Å) and **4** (3.091 Å) due to the steric bulk of trimethylacetate and benzyl groups in the carboxylate bridges. For **2**, **3** and **4** the N-Fe-N, O-Fe-N and O-Fe-O bond angles fall in the range 74.6(2)- 102.55(9)° and the N-Fe-O bond angle in the range 159.49(10) - 173.69(8)°, which deviate from the ideal octahedral angles of 90° and

180° respectively, revealing the presence of significant distortion in the iron(III) coordination geometry. A molecular model building study shows that the carboxylate bridges are very flexible.

### Electronic Spectral and Electrochemical Studies

In acetonitrile solution, all the present diiron(III) complexes **1** - **6** exhibit an intense band in the range 460–520 nm ( $\epsilon_{\text{max}}$ , 830–1640 M<sup>-1</sup> cm<sup>-1</sup>, Table 3, Figure 4), which are characteristic<sup>29,49,56</sup> of O<sup>2-</sup> → iron(III) LMCT bands in oxo-bridged diiron(III) complexes containing two carboxylate bridges. The less intense band around 700 nm corresponds to the spin forbidden ligand field (LF) transition, which is expected for the mononuclear high-spin octahedral iron(III) complexes.<sup>49</sup> The oxo-bridge of all the complexes remains intact in dichloromethane/acetonitrile solvent mixture as revealed by ESI-MS analysis.

The electrochemical properties of the diiron(III) complexes were investigated in acetonitrile/dichloromethane solvent mixture by employing cyclic (CV) and differential pulse voltammetry (DPV) on a stationary platinum electrode. All the complexes show a cathodic peak in the range -0.633 to -0.841 V in the CV, which corresponds to one electron reduction in the



diiron(III) unit, and no coupled oxidation wave is discernible (Figure 5). The  $E_{1/2}$  values of the Fe<sup>III</sup>/Fe<sup>II</sup> redox couple (-0.595 to -0.770 V, Table 3) fall in the range observed for similar type of triply-bridged diiron(III) complexes.<sup>40,48,49</sup> They are highly negative mainly due to the strong coordination of the bridging carboxylate and oxo groups and follow the trend **1** < **2** < **3** > **4** > **5** > **6** revealing the importance of the bridging carboxylates in stabilizing iron(III) oxidation state. Thus on replacing both the bridging formates ( $pK_a$ , HCOOH, 3.77) in **1** by the bridging acetates ( $pK_a$ , AcOH, 4.76) to obtain **2**, the Fe<sup>III</sup>/Fe<sup>II</sup> redox potential is shifted from -0.665 V to a more negative value (-0.757 V), which is expected of the acetate anion coordinating more strongly to iron(III) center. A similar shift in redox potential is observed on moving from **2** to **3** ( $E_{1/2}$ , -0.770 V) revealing that the stronger coordination of trimethylacetate anion ( $pK_a$ , Me<sub>3</sub>AcOH, 5.0) renders the iron(III) center difficult to reduce. However, the X-ray crystal structures of **2** and **3** show that the trimethylacetate anion binds more weakly than the acetate anion (cf. above) possibly due to the higher steric bulk of the former. On replacing the electron-releasing methyl groups in the bridging acetates in **2** by electron-withdrawing phenyl group to obtain **4**, the

Fe<sup>III</sup>/Fe<sup>II</sup> redox potential is shifted to a less negative value ( $E_{1/2}$ , -0.743 V) implying weaker coordination of benzoates ( $pK_a$ , BzOH, 4.19) to iron(III). Upon replacing both the bridging benzoates in **4** by diphenylacetates ( $pK_a$ , Ph<sub>2</sub>AcOH, 3.94) to obtain **5**, the Fe<sup>III</sup>/Fe<sup>II</sup> redox potential is shifted to a less negative value ( $E_{1/2}$ , -0.630 V) revealing that diphenylacetate ion is coordinated to iron(III) more weakly than the benzoate anion. A similar shift in redox potential is observed on moving from **5** to **6** ( $E_{1/2}$ , -0.595 V) revealing that the triphenylacetate anion ( $pK_a$ , Ph<sub>3</sub>AcOH, 3.96) coordinates less strongly to iron(III) making it easier to reduce. Thus upon replacing the electron-releasing substituents by the less electron-releasing ones, the Fe<sup>III</sup>/Fe<sup>II</sup> redox potential becomes progressively less negative revealing that a variation in the substituents on the bridging carboxylate tunes well the redox potential. In fact, interestingly, a linear correlation between the  $pK_a$  of the bridging carboxylate and  $E_{1/2}$  value is obtained (Figure 6).

### Functionalization of alkanes

The experimental conditions and results of catalytic oxidation of alkanes for the diiron(III) complexes **1-6** are summarized in Tables 4 and 5. The conversion of alkanes into hydroxylated products was quantified based on gas chromatographic analysis by using authentic samples and an internal standard. The catalytic ability of diiron(III) complexes towards oxidation of alkanes like cyclohexane and adamantane was investigated by using *m*-CPBA as oxidant in dichloromethane/acetonitrile solvent mixture (4:1 v/v) at room temperature. Control reactions performed in the absence of diiron(III) complexes with *m*-CPBA as oxidant yielded only very small amounts of oxidized products (Cyclohexane, 3 TON; Adamantane, 5 TON), revealing that all the diiron(III) complexes act as catalysts towards oxidation of alkanes to alcohols. In the presence of diiron(III) complexes the oxidation of cyclohexane proceeds to give cyclohexanol (A) as the major product along with cyclohexanone (K) and  $\epsilon$ -caprolactone as minor products. The latter is the over oxidized product of cyclohexanone in the presence of excess or unreacted *m*-CPBA. All the complexes display efficient alkane hydroxylation with 300-500 turn over numbers (TON) with good selectivity for the hydroxylation of cyclohexane (A/K, 6.0-10.1; Table 4). Also, no significant change in both product selectivity and yield is observed upon performing the reaction under nitrogen atmosphere revealing the involvement of metal based oxidants rather than radical species in the catalytic reactions. The catalytic activity of diiron(III) complexes with the same 3N capping ligand towards hydroxylation of cyclohexane follows the

trend **1** (Total TON, 401; A/K, 8.5) < **2** (442; 9.0) < **3** (492; 7.6) > **4** (411; 10.1) > **5** (398; 7.2) > **6** (387; 6.0) illustrating the importance of the bridging carboxylates. Very interestingly, the same order of TON is observed for adamantane oxidation also, **1** (Total TON, 381; 3°/2°, 15.1) < **2** (466; 14.9) < **3** (476; 17.1) > **4** (437; 15.7) > **5** (416; 13.8) > **6** (399; 12.9) (Table 5) revealing the involvement of a mechanism same as that for cyclohexane oxidation. Thus, all the present diiron(III) complexes show high selectivity in the hydroxylation of cyclohexane (A/K, 6.0–10.1; Table 4) and adamantane (3°/2°, 12.9–17.1) as well, signifying the involvement of metal-based oxidants rather than non-selective freely diffusing radical species in the alkane hydroxylation.<sup>33,37,62,63</sup> Also, recently several iron and nickel complexes have been reported involving metal-based oxidants in hydroxylation of alkanes with *m*-CPBA as oxidant.<sup>64</sup>

The complex **1** catalyses the oxidation of cyclohexane to give 408 total TON with good A/K ratio (8.5) corresponding to 51.0% conversion of the oxidant into organic products. Upon replacing both the formate bridges in **1** by acetate bridges to give **2**, the catalytic activity is enhanced to 442 total TON with the A/K ratio of 9.0 corresponding to 55% conversion. It is clear that the stronger coordination of the acetate group in **2** (cf. above) enhances the electronic charge on the iron(III) center and hence the efficiency of putative high-valent intermediate species (Scheme 5) leading to a better catalytic activity. Also, previously it has been reported that the Fe(V)=O species have been stabilized by injecting more electronic charge into the 3d shell by the strong  $\sigma$ -donating capacity of the TAML tetraanion.<sup>65</sup> Interestingly, the activity of **2** towards cyclohexane oxidation is higher than those of [Fe<sub>2</sub>O(OAc)<sub>2</sub>(<sup>*i*</sup>Bubpa/Bzbpa)<sub>2</sub>](ClO<sub>4</sub>)<sub>2</sub> (Total TON: <sup>*i*</sup>Bubpa, 380; Bzbpa, 348),<sup>33</sup> suggesting that a change in nitrogen donors of the capping ligand plays a vital role in dictating the yields of hydroxylation products of alkanes. The complex **3** catalyses the oxidation of cyclohexane with 492 total TON and A/K value of 7.6 corresponding to 62% conversion of the oxidant into the organic products, which is the highest among the present complexes and also higher than those for the previously reported triply-bridged diiron(III) complexes.<sup>29-33</sup> Upon replacing the bridging acetates in **2** by bridging trimethylacetates to obtain **3** the electron density on the iron(III) center increases (cf. above), which enhances the stability of putative high-valent intermediate species leading to higher catalytic activity. Thus, it is inferred that electron-releasing substituents on the bridging carboxylates plays a vital role in stabilizing the putative high-valent iron-oxo species formed during the catalytic cycle.

Upon replacing electron-releasing bridging acetates in **2** by electron-withdrawing benzoate groups to give **4**, a decrease in the TON (411) as well as extent of conversion (51%) but, interestingly, with a higher selectivity (A/K, 10.1) are observed. Obviously, the electron-withdrawing benzoate groups in **4** decreases the stability of putative high-valent  $\text{Fe}^{\text{IV/V}}=\text{O}$  reactive intermediate species leading to a decrease in catalytic activity. Also, a change in the capping ligand from <sup>i</sup>Bubpa/Bzbpa as in  $[\text{Fe}_2\text{O}(\text{OBz})_2(\text{Bubpa/Bzbpa})_2](\text{ClO}_4)_2$  (total TON: <sup>i</sup>Bubp, 400; Bzbpa, 329) to L in **4**, a higher total TON (411) is observed, supporting the above observation. Upon replacing both the benzoate bridging groups in **4** by diphenylacetate anions to give **5**, slightly lower total TON (398) and A/K ratio (7.3) are observed due to the incorporation of two electron-withdrawing phenyl groups in the carboxylate bridge. The diiron(III) complex **6** containing three electron-withdrawing phenyl groups in the carboxylate bridge catalyses the oxidation of cyclohexane to give total a TON of 387 with the A/K value of 6.0, which are lower than those for **5**. The electronic rather than steric effect of substituents on the bridging carboxylates play a major role in dictating the stability of intermediate species (Scheme 5) and hence the catalytic efficiency of diiron(III) complexes and in particular, the electron-releasing trimethylacetate anion in **3** makes the complex the most efficient catalyst for alkane hydroxylation reaction.

All the diiron(III) complexes catalyse the oxidation of adamantane efficiently to give 1-adamantanol and 2-adamantanol as the major products along with 2-adamantanone as the minor product. Complex **1** catalyzes the oxidation of adamantane with a total TON of 381 with a good selectivity ( $3^\circ/2^\circ$ , 15.1). Upon replacing the bridging formates in **1** by acetates to give **2**, the adamantane oxidation occurs with increased catalytic activity giving a total TON of 466, which is higher than that for **1**, as for cyclohexane oxidation (cf. above). The total TON for **3** is 476, which is the highest among the present complexes, as observed for cyclohexane oxidation. Interestingly, the replacement of methyl group on the carboxylate bridge in **2** by electron-withdrawing benzoates as in **4** leads to a total TON of 437, which is lower than that for **2**. The total TON observed for **5** is 416, which is lower than that for **4** obviously due to the higher electron-withdrawing effect of diphenylacetate bridges in the former. A still lower catalytic activity is obtained for **6** (total TON, 399), due to the presence of three electron-withdrawing phenyl groups on the bridging triphenylacetate. Also, the selectivity observed for **5** ( $3^\circ/2^\circ$ : 13.8) and **6** ( $3^\circ/2^\circ$ : **6**, 12.9) is lower than that for **4**. Thus, a variation in the substituents on the bridging

carboxylates around the diiron(III) centre leads to remarkable tuning of the catalytic efficiency towards adamantane oxidation.

Interestingly, a linear correlation is observed between the  $pK_a$  of the bridging carboxylates and total TON (Figure S2 and S3) revealing that the coordinating ability of the bridging carboxylates as determined by the substituents on them plays a vital role in determining the catalytic ability of the diiron(III) complexes. Also, there is a linear correlation between the  $E_{1/2}$  value and total TON (Figure S4), which is expected of the observed linear correlation between the  $pK_a$  of the bridging carboxylates and the  $E_{1/2}$  value of the diiron(III) complexes (cf. above). So, it is evident that the  $E_{1/2}$  value may be considered as a measure of stabilization of iron(III) oxidation state and hence that of putative high-valent intermediate species. Also, it has been previously shown that, on increasing the number of pyridyl nitrogen donors in some mononuclear iron(II) complexes, the  $Fe^{III}/Fe^{II}$  redox potential is shifted to more negative values and the negative charge built on the iron center stabilizes the high-valent iron-oxo intermediate species.<sup>62</sup> Similarly, the present diiron(III) complexes with more negative  $Fe^{III}/Fe^{II}$  redox potentials facilitate the formation of putative high-valent intermediate species so as to act as efficient turn over catalysts for alkane hydroxylation.

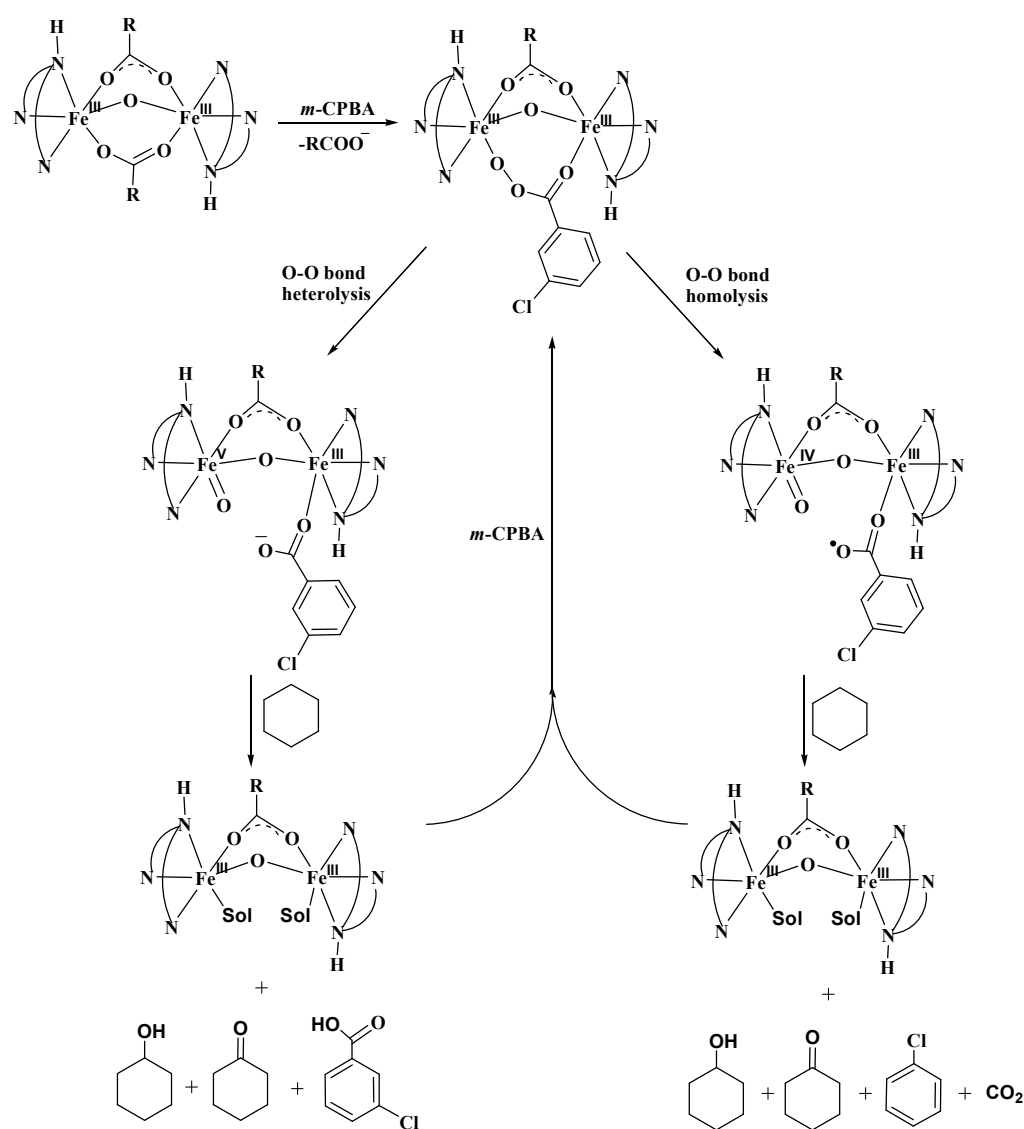
### Reaction of diiron(III) complexes with *m*-CPBA

When the oxidant  $H_2O_2$  or *t*-BuOOH is added to the diiron(III) complexes dissolved in dichloromethane/acetonitrile solvent mixture at room temperature no spectral change is observed even after adding triethylamine. Also, the addition of the strong oxidant *m*-CPBA to acetonitrile solution of the diiron(III) complexes at room temperature produces no significant spectral changes. However, addition of one equivalent of triethylamine to the reaction mixture leads to the appearance of a new band in the region of 680-720 nm (Figure 7). Previously it was reported that that the band corresponds to the formation of  $[Fe_2O(^iBubpa/Bzbpa)_2(OBz)-(OOCOC_6H_4Cl)]^{2+}$ ,<sup>33</sup> formed upon replacing one of the bridging carboxylates by *m*-CPBA. For the present adducts also no intermediate was discerned characteristic of high-valent intermediate species during their decay in the absence of any substrate. However, such an intermediate species has been proposed to be formed initially in alkane hydroxylation reactions catalyzed by the complexes  $[Fe_2(O)(OBz)_2(^iBubpa/Bzbpa)_2](ClO_4)_2$ <sup>33</sup> and  $[Fe_2(O)(OAc)_2(hexpy)](ClO_4)_2$ <sup>29</sup> using *m*-CPBA as oxidant. On the other hand, the electrospray ionization mass (ESI-MS) spectrum of

the reaction mixture of **4** with 1 eq. of *m*-CPBA and 1 eq. of TEA at RT in acetonitrile shows five peaks at  $m/z = 827.0, 860.9, 882.8, 894.9$  and  $916.8$  corresponding to  $\{[\text{Fe}_2^{\text{III}}(\text{O})(\text{L})_2(\text{OBz})_2]\text{ClO}_4\}^+$ ,  $\{[\text{Fe}_2^{\text{III}}(\text{O})(\text{L})_2(\text{OBz})_2]\text{ClO}_4\}^+$ ,  $\{[\text{Fe}_2^{\text{III}}(\text{O})(\text{L})_2(\text{OBz})(\text{OBzCl})]\text{ClO}_4\}^+$ ,  $\{[\text{Fe}_2^{\text{III}}(\text{O})(\text{L})_2(\text{OBz})_2](\text{OBzCl})\}^+$  and  $\{[\text{Fe}_2^{\text{III}}(\text{O})(\text{L})_2(\text{OBz})(\text{OBzCl})](\text{OBzCl})\}^+$  respectively. Due to the addition of *m*-CPBA the diiron(III) complex forms different cations under ESI condition. Also, the electrospray ionization mass (ESI-MS) spectrum of the reaction mixture of **4** with 5 eq. of *m*-CPBA and 1 eq. of TEA at RT in acetonitrile shows four intense peaks at  $m/z = 860.9, 894.8, 916.8$  and  $950.7$  corresponding to  $\{[\text{Fe}_2^{\text{III}}(\text{O})(\text{L})_2(\text{OBz})_2]\text{ClO}_4\}^+$ ,  $\{[\text{Fe}_2^{\text{III}}(\text{O})(\text{L})_2(\text{OBz})_2](\text{OBzCl})\}^+$ ,  $\{[\text{Fe}_2^{\text{III}}(\text{O})(\text{L})_2(\text{OBz})(\text{OBzCl})](\text{OBzCl})\}^+$  and  $\{[\text{Fe}_2^{\text{III}}(\text{O})(\text{L})_2(\text{OBzCl})_2](\text{OBzCl})\}^+$  and three less intense peaks at  $876.8, 882.8$  and  $910.8$  (Figure S1). From the observed isotope distribution patterns, the peak at  $876.8$  is formulated as  $\{[\text{Fe}_2^{\text{III}}(\text{O})(\text{L})_2(\text{OBz})(\text{OOCOC}_6\text{H}_4\text{Cl})]\text{ClO}_4\}^+$  and is derived from the diiron(III) complex resulting from the replacement of one of the benzoate bridging ligand. Such a species formation has also been reported previously for the  $[\text{Fe}_2\text{O}(\text{Bubpa}/\text{Bzbpa})_2(\text{OBz})_2]^{2+}$ .<sup>33</sup> The ESI-MS spectrum also features other less intense band at  $910.8$  is formulated as  $\{[\text{Fe}_2^{\text{III}}(\text{O})(\text{L})_2(\text{OBzCl})(\text{OOCOC}_6\text{H}_4\text{Cl})]\text{ClO}_4\}^+$  is derived from the diiron(III) complex resulting from the replacement of one of the benzoate bridging ligand by *m*-chlorobenzoic acid and the other benzoate by *m*-chloroperbenzoic acid. Also, we propose that all the other peaks are formed from the diiron(III) complex in the absence of a substrate, under the ESI-MS conditions.

So, we now propose that the acyloxo adduct species  $[\text{Fe}_2\text{O}(\text{L})_2(\text{RCO}_2)(\text{OOCOC}_6\text{H}_4\text{Cl})]^{2+}$  (Scheme 5) either undergoes O-O bond homolysis or O-O bond heterolysis leading to the formation respectively of putative high-valent  $\text{Fe}^{\text{III}}\text{-O-Fe}^{\text{IV}}\text{=O}$  or  $\text{Fe}^{\text{III}}\text{-O-Fe}^{\text{V}}\text{=O}$  intermediate species, which are involved in the selective hydroxylation of alkanes. For all the present diiron(III) complexes we have observed the formation of chlorobenzene up to 90% based on total TON. This observation strongly supports the proposed formation of the adduct species  $[\text{Fe}_2\text{O}(\text{L})_2(\text{RCO}_2)(\text{OOCOC}_6\text{H}_4\text{Cl})]^{2+}$ , undergoes O-O bond homolysis leading to generate  $\text{Fe}^{\text{III}}\text{-O-Fe}^{\text{IV}}\text{=O}$  species and chlorobenzoate radical. The chlorobenzene is formed from the decarbonylation of chlorobenzoate radical. This observation also resembles the recent observation by Que and coworkers that the mononuclear  $[(S,S\text{-PDP})\text{Fe}^{\text{III}}(\kappa^2\text{-peracetate})]$  species undergo O-O bond hemolysis to form the  $[(S,S\text{-PDP})\text{Fe}^{\text{IV}}(\text{O})(\text{AcO}^\cdot)]$  species, that performs the efficient alkane hydroxylation.<sup>63</sup> As chlorobenzene is produced up to 90% based on total TON, it

has been suggested that up to 90% of the oxidized products are formed from the involvement of putative high-valent  $\text{Fe}^{\text{III}}\text{-O-Fe}^{\text{IV}}\text{=O}$  species. Also, recently Que and coworkers characterized the similar intermediate species, derived from the diiron(III) complex  $[\text{Fe}^{\text{III}}_2\text{O(L)}_2]^{2+}$ , where L is *N,N*-bis-(3',5'-dimethyl-4'-methoxypyridyl-2'-methyl)-*N'*-acetyl-1,2-diaminoethane.<sup>66</sup> Also, Wieghardt and co-workers have reported the formation of  $\text{Fe}^{\text{III}}\text{-O-Fe}^{\text{IV}}\text{=O}$  species derived by one electron oxidation of  $(\mu\text{-oxo})\text{bis}(\mu\text{-carboxylato})\text{diiron(III)}$  complexes.<sup>67</sup> In addition, chlorobenzene is only produced up to 90% based on the total TON. So, it is clear that some other intermediate species is also involved in the hydroxylation reaction to produce the remaining



**Scheme 5.** Proposed mechanism for alkane hydroxylation

hydroxylated products. So, we also propose the involvement of putative high-valent Fe<sup>III</sup>-O-Fe<sup>V</sup>=O species responsible for the hydroxylation of the remaining hydroxylated products, which may be formed from the O-O bond heterolysis of the acyloxo adduct species, favored by the electron-releasing bridging carboxylates.

## Conclusions

A series of non-heme  $\mu$ -oxo- and bis( $\mu$ -carboxylato)-bridged diiron(III) complexes of a linear 3N ligand has been isolated and all of them possess distorted bioctahedral geometry around the diiron(III) centre. The good selectivity observed for cyclohexane hydroxylation using *m*-CPBA as oxidant (A/K, 6.0-10.1) and adamantane (3°/2°, 12.9-17.1) suggests the involvement of putative high-valent iron-oxo species rather than freely diffusing radicals in the catalytic reaction. Interestingly, the total TON observed for hydroxylation of cyclohexane for the diiron(III) complexes with trimethylacetate bridges is the highest among the present complexes and is also higher than those observed for the previously reported triply-bridged diiron(III) complexes. Also, interestingly, the incorporation of electron-releasing substituents on the carboxylate bridges makes the diiron(III) complex to an efficient catalyst towards alkane hydroxylation whereas that of electron-withdrawing substituents makes the complex a relatively poor catalyst. Thus, an interesting linear correlation between the TON of the diiron(III) complexes and  $pK_a$  of the bridging carboxylates has been observed, which reveals that electronic rather than steric effect of the substituents on bridging carboxylates plays a remarkable role in dictating the efficiency as well as selectivity of catalysts towards alkane hydroxylation.

## Acknowledgments

We sincerely thank the Department of Science and Technology, New Delhi for DST a Nano Mission Project [Scheme No. SR/NM/NS-110/2010(G) for funding with a Research Associateship (M.B.) and SERB, New Delhi for a research project EMR/2015/002222.

## References

1. J. Colby, H. Dalton and R. Whittenbury, *Annu. Rev. Microbiol.*, 1979, **33**, 481.
2. H. Dalton, *Adv. Appl. Microbiol.*, 1980, **26**, 7.
3. J. B. Vincent, G. L. Olivier-Lilley and B. A. Averill, *Chem. Rev.*, 1990, **90**, 1447.
4. J. D. Lipscomb, *Annu. Rev. Microbiol.*, 1994, **48**, 317.
5. A. L. Feig and S. J. Lippard, *Chem. Rev.*, 1994, **94**, 759
6. B. J. Waller and J. D. Lipscomb, *Chem. Rev.*, 1996, **96**, 2625.
7. M. Baik, M. Newcomb, R. A. Friesner and S. J. Lippard, *Chem. Rev.*, 2003, **103**, 2385.
8. M. Costas, M. P. Mehn, M. P. Jensen and L. Que Jr., *Chem. Rev.* 2004, **104**, 939.
9. E. Y. Tshuva and S. J. Lippard, *Chem. Rev.*, 2004, **104**, 987.
10. S. V. Kryatov, E. V. Rybak-Akimova and S. Schindler, *Chem. Rev.*, 2005, **105**, 2175.
11. D. Riley, M. Stern and J. Ebner, in *The Activation of Dioxygen and Homogeneous Catalytic Oxidation*, ed. D. H. R. Barton, A. E. Martell and D. T. Sawyer, Plenum, New York, 1993, p. 31.
12. (a) M. Merckx, D. A. Kopp, M. H. Sazinsky, J. L. Blazyk, J. Muller and S. J. Lippard, *Angew. Chem., Int. Ed.*, 2001, **40**, 4000. (b) A. C. Rosenzweig, C. A. Frederick, S. J. Lippard and P. Nordlund, *Nature*, 1993, **366**, 537. (c) L. Westerheide, M. Pascaly and B. Krebs, *Curr. Opin. Chem. Biol.*, 2000, **4**, 235.
13. (a) A. Jordan and P. Reichard, *Annu. Rev. Biochem.*, 1998, **67**, 71. (b) D. T. Logan, X. -D. Su, A. Aberg, K. Regnstrom, J. Hajdu, H. Eklund and P. Nordlund, *Structure*, 1996, **4**, 1053. (c) J. Stubbe, *Curr. Opin. Chem. Biol.*, 2003, **7**, 183.
14. R. E. Stenkamp, *Chem. Rev.*, 1994, **94**, 715.
15. (a) E. I. Solomon, F. Tucek, D. E. Root and C. A. Brown, *Chem. Rev.*, 1994, **94**, 827. (b) D. M. Kurtz, Jr., *Chem. Rev.*, 1990, **90**, 585.
16. (a) J. B. Vincent, G. L. Oliver-Lilley and B. A. Averill, *Chem. Rev.*, 1990, **90**, 1447. (b) S. J. Lippard, *Angew. Chem., Int. Ed. Engl.*, 1988, **27**, 344.
17. P. C. Wilkins and R. C. Wilkins, *Coord. Chem. Rev.*, 1987, **79**, 195.
18. S. V. Kryatov, E. V. Rybak-Akimova and S. Schindler, *Chem. Rev.*, 2005, **105**, 2175.

19. (a) K. Chen and L. Que, Jr., *Chem. Commun.*, 1999, 1375. (b) K. Chen and L. Que, Jr., *J. Am. Chem. Soc.*, 2001, **123**, 6327. (c) Y. Mekmouche, S. Ménage, C. Toia-Duboc, M. Fontecave, J.-B. Galey, C. Lebrun and J. Pécaut, *Angew. Chem., Int. Ed.*, 2001, **40**, 949. (d) K. Chen and L. Que Jr., *Angew. Chem., Int. Ed.*, 1999, **38**, 2227. (e) W. Nam, R. Ho and J. S. Valentine, *J. Am. Chem. Soc.*, 1991, **113**, 7052. (f) K. Chen, M. Costas and L. Que, Jr., *J. Chem. Soc., Dalton Trans.*, 2002, 672.
20. M. Fontecave, S. Ménage and C. Duboc-Toia, *Coord. Chem. Rev.*, 1998, **178**, 1555.
21. W. H. Armstrong and S. J. Lippard, *J. Am. Chem. Soc.*, 1983, **105**, 4837.
22. K. Wieghardt, I. Tolksdorf and W. Herrmann, *Inorg. Chem.*, 1985, **24**, 1230.
23. K. Wieghardt, K. Pohl and W. Gebert, *Angew. Chem., Int. Ed. Engl.*, 1983, **22**, 727.
24. K. B. Jensen, C. J. McKenzie, O. Simonsen, H. Toftlund and A. Hazell, *Inorg. Chim. Acta*, 1997, **257**, 163.
25. S. Nishino, H. Hosomi, S. Ohba, H. Matsushima, T. Tokii and Y. Nishida, *J. Chem. Soc., Dalton Trans.*, 1999, 1509.
26. J. B. Vincent, J. C. Huffmann, G. Christou, Q. Li, M. A. Nanny, D. N. Hendrickson, R. H. Fong and R. H. Fish, *J. Am. Chem. Soc.*, 1988, **110**, 6898.
27. R. H. Fish, M. S. Konings, K. J. Oberhausen, R. H. Fong, W. M. Yu, G. Christou, J. B. Vincent, D. K. Coggin and R. M. Buchanan, *Inorg. Chem.*, 1991, **30**, 3002.
28. N. Kitajima, H. Fukui and Y. Moro-oka, *J. Chem. Soc., Chem. Commun.*, 1988, 485.
29. M. Kodera, H. Shimakoshi and K. Kano, *Chem. Commun.*, 1996, 1737.
30. M. Kodera, H. Shimakoshi, M. Nishimura, H. Okawa, S. Iijima and K. Kano, *Inorg. Chem.*, 1996, **35**, 4967.
31. M. Kodera, Y. Taniike, M. Itoh, Y. Tanahashi, H. Shimakoshi, K. Kano, S. Hirota, S. Iijima, M. Ohba and H. Okawa, *Inorg. Chem. Commun.*, 2001, **40**, 4821.
32. M. Itoh, M. Kodera and K. Kano, *J. Inorg. Biochem.*, 2003, **96**, 158.
33. K. Visvaganesan, E. Suresh and M. Palaniandavar, *Dalton Trans.*, 2009, 3814.
34. R. M. Buchanan, S. Chen, J. F. Richardson, M. Bressan, L. Forti, A. Morvillo and R. H. Fish, *Inorg. Chem.*, 1994, **33**, 3208.
35. D. Tetard and J.-B. Verlhac, *J. Mol. Catal. A: Chem.*, 1996, **113**, 223.

36. (a) R. E. Norman, S. Yan, L. Que, Jr., G. Backes, J. Ling, J. Sanders-Loehr, J. H. Zhang and C. J. O'Connor, *J. Am. Chem. Soc.*, 1990, **112**, 1554 (b) R. A. Leising, J. Kim, M. A. Pérez and L. Que, Jr., *J. Am. Chem. Soc.*, 1993, **115**, 9524.
37. I. W. C. E. Arends, K. U. Ingold and D. D. M. Wayner, *J. Am. Chem. Soc.*, 1995, **117**, 4710.
38. R. H. Fish, M. S. Konings, K. J. Oberhausen, R. H. Fong, W. M. Yu, G. Christou, J. B. Vincent, D. K. Coggin and R. M. Buchanan, *Inorg. Chem.*, 1991, **30**, 3002.
39. T. Okuno, S. Itoh, S. Ohba and Y. Nishida, *J. Chem. Soc., Dalton Trans.*, 1997, 3547.
40. S. Ménage, J.-B. Galey, J. Dumats, G. Hussler, M. Seite', I. G. Luneau, G. Chottard and M. Fontecave, *J. Am. Chem. Soc.*, 1998, **120**, 13370.
41. A. Raja, V. Rajendiran, P. Uma Maheswari, R. Balamurugan, C. A. Kilner, M. A. Halkrow and M. Palaniandavar, *J. Inorg. Biochem.*, 2005, **99**, 1717.
42. (a) G. M. Sheldrick, *SHELXTL Reference Manual: Version 5.1*; Bruker AXS: Madison, WI, 1997. (b) O. V. Dolomanov, L. J. Bourhis, R. J. Gildea, J. A. K. Howard and H. Puschmann. "OLEX2: a complete structure solution, refinement and analysis program". *J. Appl. Cryst.* 2009, **42**, 339- 341.
43. (a) SMART & SAINT Software References manuals, version 5.0; Bruker AXS Inc.: Madison, WI, 1998. (b) G. M. Sheldrick, *SHELXL-97: Program for Crystal Structure Refinement*; University of Göttingen: Göttingen, Germany, 1997.
44. (a) G. M. Sheldrick, SAINT 5.1 eds. Siemens Industrial Automation Inc.: Madison, WI, 1995. (b) G. M. Sheldrick, *Acta Crystallogr.* 2008, **A64**, 112–122.
45. (a) *SADABS, empirical absorption Correction Program*; University of Göttingen: Göttingen, Germany, 1997. ) (b) A. L. Spek, *J. Appl. Crystallogr.* 2003, **36**, 7. (c) P. van der Sluis, A. L. Spek, *Acta Crystallogr., Sect. A: Found. Crystallogr.* 1990, **46**, 194.
46. P. Chaudhuri, K. Wieghardt, B. Nuber and J. Weiss, *Angew. Chem., Int. Ed. Engl.*, 1985, **24**, 778.
47. (a) K. Wieghardt, K. Pohl and D. Ventur, *Angew. Chem., Int. Ed. Engl.*, 1985, **24**, 392. (b) U. Bossek, H. Hummel, T. Weyhermüller, E. Bill and K. Wieghardt, *Angew. Chem., Int. Ed. Engl.* 1995, **34**, 2642.
48. J.-A. R. Hartman, R. L. Rardin, P. Chaudhuri, K. Pohl, K. Wieghardt, B. Nuber, J. Weiss, G. C. Papaefthymiou, R. B. Frankel and S. J. Lippard, *J. Am. Chem. Soc.*, 1987, **109**, 7387

49. W. H. Armstrong, A. Spool, G. C. Papaefthymiou, R. B. Frankel and S. J. Lippard, *J. Am. Chem. Soc.*, 1984, **106**, 3653.
50. A. Spool, I. D. Williams and S. J. Lippard, *Inorg. Chem.*, 1985, **24**, 2156.
51. (a) K. Visvaganesan, R. Mayilmurugan, E. Suresh and M. Palaniandavar, *Inorg. Chem.* 2007, **46**, 10294. (b) K. Sundaravel, T. Dhanalakshmi, E. Suresh and M. Palaniandavar, *Dalton Trans.*, 2008, 7012. (c) M. Velusamy, R. Mayilmurugan and M. Palaniandavar, *Inorg. Chem.* 2004, **43**, 6284. (d) R. Mayilmurugan, K. Visvaganesan, E. Suresh and M. Palaniandavar, *Inorg. Chem.* 2009, **48**, 8771. (e) R. Mayilmurugan, E. Suresh and M. Palaniandavar, *Inorg. Chem.* 2007, **46**, 6038. (f) K. Sundaravel, M. Sankaralingam, E. Suresh and M. Palaniandavar, *Dalton Trans.*, 2011, **40**, 8444. (g) K. Sundaravel, E. Suresh, K. Saminathan and M. Palaniandavar, *Dalton Trans.*, 2011, **40**, 8092. (h) R. Viswanathan, M. Palaniandavar, T. Balasubramanian and T. P. Muthiah, *Inorg. Chem.*, 1998, **37(12)**, 2943.
52. T. Kojima, R. A. Leising, S. Yan and L. Que Jr., *J. Am. Chem. Soc.* 1993, **115**, 11328.
53. W. M. Reiff, T. F. Brennan and A. R. Garofalo, *Inorg. Chim. Acta*, 1983, **77**, L83.
54. K. Dehnicke, H. Prinz, W. Massa, J. Pebler and R. Z. Z. Schmidt, *Anorg. Allg. Chem.*, 1983, **499**, 20.
55. (a) K. B. Jensen, C. J. McKenzie, O. Simonsen, H. Toftlund and A. Hazell, *Inorg. Chim. Acta*, 1997, **257**, 163. (b) J. Qian, Q. Wang, W. Gu, J. Tian, S. Yan, D. Liao and P. Cheng, *Transition Metal Chemistry*, 2007, **32**, 847.
56. P. Gomez-Romero, N. Casan-Pastor, A. Ben-Hussein and G. B. Jameson, *J. Am. Chem. Soc.*, 1988, **110**, 1988.
57. (a) S. Ito, T. Okuno, H. Matsushima, T. Tokii and Y. Nishida, *J. Chem. Soc., Dalton Trans.*, 1996, 4037. (b) J. Mukherjee, V. Balamurugan, R. Gupta and R. Mukherjee, *Dalton Trans.*, 2003, 3483.
58. M. G. B. Drew, V. McKee and S. M. Nelson, *J. Chem. Soc., Dalton Trans.*, 1978, 80.
59. H. Schmidbaur, C. E. Zybilla and D. Neugebauer, *Angew. Chem., Int. Ed. Engl.*, 1983, **22**, 156 and 161.
60. (a) W. H. Armstrong, A. Spool, G. C. Papaefthymiou, R. B. Frankel and S. J. Lippard, *J. Am. Chem. Soc.*, 1984, **106**, 3653. (b) G. Dubois, A. Murphy and T. D. P. Stack, *Org. Lett.*, 2003, **5**, 2469. (c) S. Ménage, J. M. Vincent, C. Lambeaux, G. Chottard, A. Grand and M. Fontecave, *Inorg. Chem.*, 1993, **32**, 4766. (d) C. Marchi-Delapierre, A. Jorge-Robin, A. Thibon and S. Ménage, *Chem. Commun.*, 2007, 1166. (e) I. Tabushi, T. Nakajima and K. Seto, *Tetrahedron Lett.*, 1980, **21**, 2565.

61. (a) R. V. Thundathil, E. M. Holt, S. L. Holt and K. J. Watson, *J. Am. Chem. Soc.*, 1977, **99**, 1818. (b) M. C. White, A. G. Doyle and E. N. Jacobsen, *J. Am. Chem. Soc.* 2001, **123**, 7194. (c) S. Menage, J-B. Galey, G. Hussler, M. Seite and M. Fontecave, *Angew. Chem. Int. Ed. Engl.* 1996, **35**, 2353. (d) S. V. Kryatov, S. Taktak, I. V. Korendovych and E. V. Rybak-Akimova, J. Kaizer, S. Torelli, X. Shan, S. Mandal, V. L. MacMurdo, A. M. Payeras and L. Que, Jr., *Inorg. Chem.* 2005, **44**, 85.
62. J. Kaizer, E. J. Klinker, N. Y. Ho, J.-U. Rohde, W. J. Song, A. Stubna, J. Kim, E. Münck, W. Nam and L. Que, Jr., *J. Am. Chem. Soc.*, 2004, **126**, 472.
63. Y. Wang, D. Janardanan, D. Usharani, K. Han, L. Que, Jr. and S. Shaik, *ACS Catal.* 2013, **3**, 1334.
64. (a) A. N. Biswas, P. Das, A. Agarwala, D. Bandyopadhyay, P. Bandyopadhyay, *J. Mol. Cat. A: Chem.* 2010, **326**, 94. (b) E. Tordin, M. List, U. Monkowius, S. Schindler, G. Knör, *Inorg. Chim. Acta*, 2013, **402**, 90. (c) A. Kejriwal, A. N. Biswas, A. Choudhury, P. Bandyopadhyay, *Trans. Met. Chem.* 2014, **39**, 909. (d) T. Nagataki, Y. Tachi, S. Itoh, *Chem. Commun.* 2006, 4016. (e) T. Nagataki, K. Ishii, Y. Tachi, S. Itoh, *Dalton Trans.* 2007, 1120. (f) T. Nagataki, S. Itoh, *Chem. Lett.* 2007, **36 (6)**, 748. (g) M. Balamurugan, R. Mayilmurugan, E. Suresh, M. Palaniandavar, *Dalton Trans.* 2011, **40**, 9413. (h) M. Sankaralingam, P. Vadivelu, E. Suresh, M. Palaniandavar, *Inorg. Chim. Acta*, 2013, **407**, 98. (i) S. Hikichi, K. Hanaue, T. Fujimura, H. Okuda, J. Nakazawa, Y. Ohzu, C. Kobayashi, M. Akita, *Dalton Trans.*, 2013, **42**, 3346. (j) M. Sankaralingam, M. Balamurugan, M. Palaniandavar, P. Vadivelu, C. H. Suresh, *Chem. Eur. J.* 2014, **20**, 11346. (k) D. D. Narulkar, A. R. Patil, C. C. Naik, S. N. Dhuri, *Inorg. Chim. Acta*, 2015, **427**, 248.
65. F. T. Oliveira, A. Chanda, D. Banerjee, X. Shan, S. Mondal, Jr., L. Que, E. L. Bominaar, E. Munch and T. J. Collins, *Science*, 2007, **315**, 835.
66. D. Wang, E. R. Farquhar, A. Stubna, E. Münck and L. Que, Jr. *Nat. Chem.* 2009, **1**, 145.
67. L. D. Slep, A. Mijovilovich, W. Meyer-Klaucke, T. Weyhermüller, E. Bill, E. Bothe, F. Neese and K. Wieghardt, *J. Am. Chem. Soc.* 2003, **125**, 15554.

**Table 1.** Crystal Data and Structure Refinement Details for [Fe<sub>2</sub>O(OAc)<sub>2</sub>(L1)<sub>2</sub>](ClO<sub>4</sub>)<sub>2</sub> **2**, [Fe<sub>2</sub>O(Me<sub>3</sub>Ac)<sub>2</sub>(L2)<sub>2</sub>](ClO<sub>4</sub>)<sub>2</sub>·CH<sub>3</sub>CN **3** and [Fe<sub>2</sub>O(OBz)<sub>2</sub>(L1)<sub>2</sub>](ClO<sub>4</sub>)<sub>2</sub>·CH<sub>3</sub>OH·H<sub>2</sub>O **4**

	<b>2</b>	<b>3</b>	<b>4</b>
Empirical formula	C <sub>24</sub> H <sub>42</sub> Fe <sub>2</sub> N <sub>6</sub> O <sub>13</sub> Cl <sub>2</sub>	C <sub>32</sub> H <sub>55</sub> Fe <sub>2</sub> N <sub>7</sub> O <sub>13</sub> Cl <sub>2</sub>	C <sub>35</sub> H <sub>50</sub> Fe <sub>2</sub> N <sub>6</sub> O <sub>15</sub> Cl <sub>2</sub>
Formula weight / g mol <sup>-1</sup>	805.22	928.43	977.41
Crystal habit, colour	Blocks, Wine Red	Blocks, Brown	Prism, Brown
Crystal system	Monoclinic	Orthorhombic	Monoclinic
Crystal size	0.50 x 0.43 x 0.34 mm	0.41 x 0.38 x 0.22 mm	0.10 x 0.10 x 0.12 mm
Space group	C2/c	P212121	C2/c
<i>a</i> , Å	25.674(10)	10.9602(7)	34.8958(8)
<i>b</i> , Å	7.876(3)	18.5001(12)	11.1865(2)
<i>c</i> , Å	20.102(8)	20.8260(14)	28.5616(7)
<i>α</i> , deg	90.00	90.00	90.00
<i>β</i> , deg	123.068(10)	90.00	127.463(2)
<i>γ</i> , deg	90.00	90.00	90
<i>V</i> /Å <sup>3</sup>	3407(2)	4222.8(5)	8849.8(3)
<i>Z</i>	8	4	8
<i>ρ</i> <sub>calcd</sub> /g cm <sup>-3</sup>	1.566	1.460	1.395
F(000)	1664	1944	3856
T/K	293	100	296
No. of Reflections collected	13280	25416	73976
No. of unique reflections	3897	9827	8138
Radiation(MoKα)/ Å	0.71073	0.71073	0.71073
Goodness-of-fit on F <sup>2</sup>	1.019	1.061	1.034
Number of refined Parameters	256	524	559
<i>R</i> <sub>1</sub> / w <i>R</i> <sub>2</sub> [ <i>I</i> >2σ( <i>I</i> )] <sup>a</sup>	0.0465/0.1243	0.0456/0.1096	0.0613/ 0.1957
<i>R</i> <sub>1</sub> / w <i>R</i> <sub>2</sub> (all data)	0.0685/0.1423	0.0508/0.1143	0.1035

$$^a R_1 = [\Sigma(|F_o| - |F_c|) / \Sigma |F_o|]; wR_2 = \{[\Sigma(w(F_o^2 - F_c^2)^2) / \Sigma(wF_o^4)]^{1/2}\}$$

**Table 2.** Selected bond lengths [ $\text{\AA}$ ] and bond angles [ $^\circ$ ] for **2**, **3** and **4**

<b>2</b>		<b>3</b>		<b>4</b>	
Bond lengths/ $\text{\AA}$					
Fe(1)-N(1)	2.202(2)	Fe(1)-N(1)	2.145(3)	Fe(1)-N(1)	2.148(4)
Fe(1)-N(2)	2.170(3)	Fe(1)-N(2)	2.192(3)	Fe(1)-N(2)	2.219(4)
Fe(1)-N(3)	2.234(3)	Fe(1)-N(3)	2.216(3)	Fe(1)-N(3)	2.203(4)
Fe(1)-O(1)	1.7913(16)	Fe(1)-O(5)	1.796(2)	Fe(1)-O(1)	1.788(3)
Fe(1)-O(2)	1.988(2)	Fe(1)-O(2)	2.069(2)	Fe(1)-O(2)	2.039(3)
Fe(1)-O(3)	2.069(2)	Fe(1)-O(3)	2.037(2)	Fe(1)-O(5)	2.001(3)
		Fe(2)-N(4)	2.159(3)	Fe(2)-N(4)	2.158(5)
		Fe(2)-N(5)	2.181(3)	Fe(2)-N(5)	2.198(5)
		Fe(2)-N(6)	2.225(3)	Fe(2)-N(6)	2.192(4)
		Fe(2)-O(5)	1.792(2)	Fe(2)-O(1)	1.794(3)
		Fe(2)-O(1)	2.021(2)	Fe(2)-O(3)	2.029(3)
		Fe(2)-O(4)	2.068(2)	Fe(2)-O(4)	2.057(3)
Bond angles/ $^\circ$					
O(1)-Fe(1)-O(2)	98.98(8)	O(5)-Fe(1)-O(3)	101.31(9)	O(1)-Fe(1)-O(5)	100.51(14)
O(1)-Fe(1)-O(3)	95.08(8)	O(5)-Fe(1)-O(2)	99.95(9)	O(1)-Fe(1)-O(2)	98.14(13)
O(2)-Fe(1)-O(3)	97.36(10)	O(3)-Fe(1)-O(2)	86.61(10)	O(2)-Fe(1)-O(5)	90.30(14)
O(1)-Fe(1)-N(2)	98.43(10)	O(5)-Fe(1)-N(1)	96.52(10)	O(1)-Fe(1)-N(1)	98.47(15)
O(2)-Fe(1)-N(2)	161.45(10)	O(3)-Fe(1)-N(1)	161.72(9)	O(5)-Fe(1)-N(1)	160.62(16)
O(3)-Fe(1)-N(2)	87.41(11)	O(2)-Fe(1)-N(1)	86.34(10)	O(2)-Fe(1)-N(1)	83.15(14)
O(1)-Fe(1)-N(1)	173.69(8)	O(5)-Fe(1)-N(2)	170.54(11)	O(1)-Fe(1)-N(3)	97.60(16)
O(2)-Fe(1)-N(1)	87.26(9)	O(3)-Fe(1)-N(2)	87.26(10)	O(5)-Fe(1)-N(3)	88.13(16)
O(3)-Fe(1)-N(1)	83.18(9)	O(2)-Fe(1)-N(2)	84.41(10)	O(2)-Fe(1)-N(3)	164.20(16)
N(2)-Fe(1)-N(1)	75.47(10)	N(1)-Fe(1)-N(2)	75.28(11)	N(1)-Fe(1)-N(3)	93.23(16)
O(1)-Fe(1)-N(3)	89.99(10)	O(5)-Fe(1)-N(3)	96.35(10)	O(1)-Fe(1)-N(2)	172.18(16)
O(2)-Fe(1)-N(3)	92.81(11)	O(3)-Fe(1)-N(3)	87.45(10)	O(5)-Fe(1)-N(2)	86.59(17)
O(3)-Fe(1)-N(3)	167.78(9)	O(2)-Fe(1)-N(3)	163.46(10)	O(2)-Fe(1)-N(2)	84.97(15)
N(2)-Fe(1)-N(3)	80.84(11)	N(1)-Fe(1)-N(3)	94.65(10)	N(1)-Fe(1)-N(2)	74.70(17)

N(1)-Fe(1)-N(3)	90.58(10)	N(2)-Fe(1)-N(3)	79.90(11)	N(3)-Fe(1)-N(2)	79.25(17)
Fe(1)-O(1)-Fe(1)	120.27(16)	O(5)-Fe(2)-O(1)	102.55(9)	O(1)-Fe(2)-O(3)	99.78(14)
		O(5)-Fe(2)-O(4)	100.03(9)	O(1)-Fe(2)-O(4)	98.03(14)
		O(1)-Fe(2)-O(4)	85.32(9)	O(3)-Fe(2)-O(4)	89.09(13)
		O(5)-Fe(2)-N(4)	97.66(10)	O(1)-Fe(2)-N(4)	99.1(2)
		O(1)-Fe(2)-N(4)	159.49(10)	O(3)-Fe(2)-N(4)	160.0(2)
		O(4)-Fe(2)-N(4)	87.75(9)	O(4)-Fe(2)-N(4)	81.70(16)
		O(5)-Fe(2)-N(5)	170.61(10)	O(1)-Fe(2)-N(6)	96.78(16)
		O(1)-Fe(2)-N(5)	85.04(10)	O(3)-Fe(2)-N(6)	89.17(16)
		O(4)-Fe(2)-N(5)	85.97(9)	O(4)-Fe(2)-N(6)	165.17(16)
		N(4)-Fe(2)-N(5)	75.22(10)	N(4)-Fe(2)-N(6)	95.21(18)
		O(5)-Fe(2)-N(6)	94.68(10)	O(1)-Fe(2)-N(5)	172.34(17)
		O(1)-Fe(2)-N(6)	85.48(9)	O(3)-Fe(2)-N(5)	87.02(16)
		O(4)-Fe(2)-N(6)	164.04(10)	O(4)-Fe(2)-N(5)	85.51(16)
		N(4)-Fe(2)-N(6)	96.44(10)	N(4)-Fe(2)-N(5)	74.6(2)
		N(5)-Fe(2)-N(6)	80.27(10)	N(6)-Fe(2)-N(5)	79.69(18)
		Fe(1)-O(5)-Fe(2)	116.96(11)	Fe(1)-O(1)-Fe(2)	119.32(16)

---

**Table 3.** UV-Visible spectral data and electrochemical data of the diiron(III) complexes in DCM:ACN mixture at 25 °C

Complex	$\lambda_{\max}/\text{nm}$ ( $\epsilon/\text{M}^{-1} \text{cm}^{-1}$ )	$E_{\text{p,c}}$ (CV) (V)	$E_{1/2}$ (DPV) (V)	Redox Process
$[\text{Fe}_2(\text{O})(\text{OOCH})_2(\text{L})]^{2+}$ <b>1</b>	468 (1640) 511 (1060) 713 (215)	-0.713	-0.665	$\text{Fe}^{\text{III}}\text{Fe}^{\text{III}} \rightarrow \text{Fe}^{\text{II}}\text{Fe}^{\text{III}}$
$[\text{Fe}_2(\text{O})(\text{OAc})_2(\text{L})]^{2+}$ <b>2</b>	466 (1413) 506 (1153) 713 (230)	-0.825	-0.757	$\text{Fe}^{\text{III}}\text{Fe}^{\text{III}} \rightarrow \text{Fe}^{\text{II}}\text{Fe}^{\text{III}}$
$[\text{Fe}_2(\text{O})(\text{Me}_3\text{Ac})_2(\text{L})]^{2+}$ <b>3</b>	464 (1236) 507 (929) 713 (134)	-0.841	-0.770	$\text{Fe}^{\text{III}}\text{Fe}^{\text{III}} \rightarrow \text{Fe}^{\text{II}}\text{Fe}^{\text{III}}$
$[\text{Fe}_2(\text{O})(\text{OBz})_2(\text{L})]^{2+}$ <b>4</b>	466 (1445) 507 (1108) 720 (171)	-0.743	-0.679	$\text{Fe}^{\text{III}}\text{Fe}^{\text{III}} \rightarrow \text{Fe}^{\text{II}}\text{Fe}^{\text{III}}$
$[\text{Fe}_2(\text{O})(\text{Ph}_2\text{Ac})_2(\text{L})]^{2+}$ <b>5</b>	467 (1090) 509 (940) 713 (150)	-0.695	-0.630	$\text{Fe}^{\text{III}}\text{Fe}^{\text{III}} \rightarrow \text{Fe}^{\text{II}}\text{Fe}^{\text{III}}$
$[\text{Fe}_2(\text{O})(\text{Ph}_3\text{Ac})_2(\text{L})]^{2+}$ <b>6</b>	466 (1028) 510 (832) 685 (144)	-0.633	-0.595	$\text{Fe}^{\text{III}}\text{Fe}^{\text{III}} \rightarrow \text{Fe}^{\text{II}}\text{Fe}^{\text{III}}$

Potential measured vs. Ag/AgNO<sub>3</sub> (0.001 M, 0.1 M TBAP); add 0.544 V to convert to NHE.

**Table 4.** Products of oxidation of cyclohexane catalyzed<sup>a</sup> by diiron(III) complexes

Complex	Cyclohexane (TON)			Total TON <sup>c</sup>	Chloro- benzene (TON)	A/K <sup>d</sup>	Yield <sup>e</sup>
	-ol <sup>b</sup>	-one <sup>b</sup>	ε-caprolactone				
<b>1</b>	365	28	15	408 ± 2	366	8.5	51.0
<b>2</b>	398	26	18	442 ± 2	390	9.0	55.2
<b>3</b>	435	30	27	492 ± 1	439	7.6	61.5
<b>4</b>	374	23	14	411 ± 2	370	10.1	51.3
<b>5</b>	350	25	23	398 ± 3	355	7.3	49.7
<b>6</b>	332	30	25	387 ± 2	349	6.0	48.3

<sup>a</sup> Reaction conditions: Catalyst ( $1 \times 10^{-3}$  mmol dm<sup>-3</sup>), Substrate (3 mol dm<sup>-3</sup>), Oxidant (0.8 mol dm<sup>-3</sup>) in DCM:ACN solvent mixture (4:1 v/v); <sup>b</sup> -ol = cyclohexanol and -one = cyclohexanone; <sup>c</sup> Total TON = no. of mmol of product/no. of mmol of catalyst; <sup>d</sup> A/K = TON of -ol/ (TON of -one + TON of ε-caprolactone); <sup>e</sup> Yield based on the oxidant.

**Table 5.** Products of oxidation of adamantane catalyzed<sup>a</sup> by diiron(III) complexes

Complex	Adamantane (TON)			Total TON <sup>c</sup>	Selectivity <sup>d</sup> 3°/2°	Yield <sup>e</sup>
	1-adol <sup>b</sup>	2-adol <sup>b</sup>	2-adone <sup>b</sup>			
<b>1</b>	318	49	14	381 ± 1	15.1	63.5
<b>2</b>	388	64	14	466 ± 2	14.9	77.6
<b>3</b>	405	56	15	476 ± 2	17.1	79.3
<b>4</b>	367	58	12	437 ± 2	15.7	72.8
<b>5</b>	342	61	13	416 ± 2	13.8	69.3
<b>6</b>	324	56	19	399 ± 2	12.9	66.0

<sup>a</sup> Reaction conditions: Catalyst ( $1 \times 10^{-3}$  mmol dm<sup>-3</sup>), Substrate (1 mol dm<sup>-3</sup>), Oxidant (0.6 mol dm<sup>-3</sup>) in DCM:ACN solvent mixture (4:1 v/v); <sup>b</sup> 1-adol = 1-adamantanol, 2-adol = 2-adamantanol and 2-adone = 2-adamantanone; <sup>c</sup> TON = no. of mmol of product/no. of mmol of catalyst; <sup>d</sup> 3°/2° = (TON of 1-adol×3)/(TON of 2-adol+ TON of 2-adone); <sup>e</sup> Yield based on the oxidant.

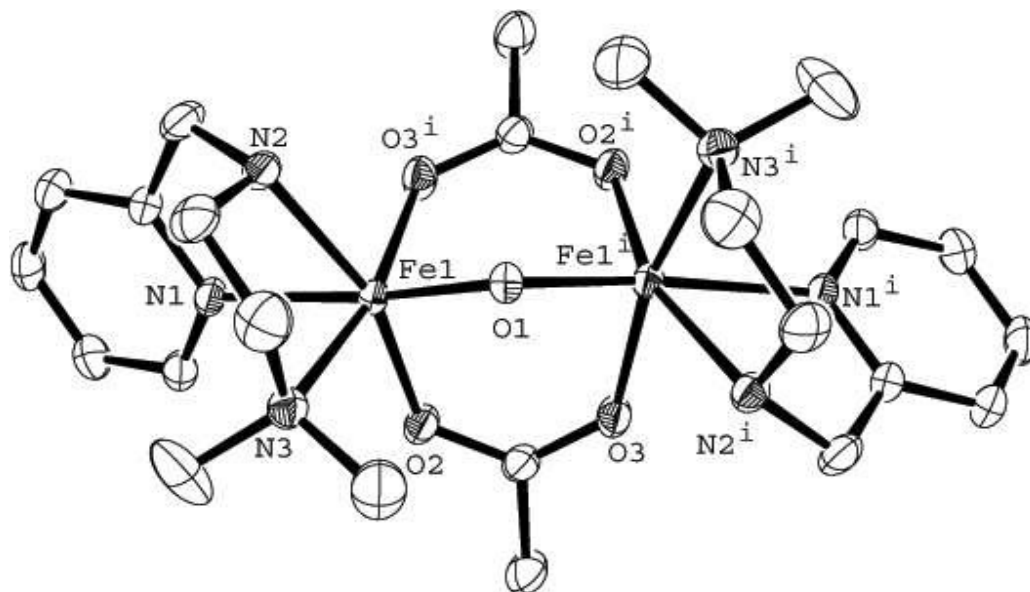


**Figure 1.** Molecular structure of  $[\text{Fe}_2\text{O}(\text{L})_2(\text{OAc})_2](\text{ClO}_4)_2$  **2** (30% probability factor for the thermal ellipsoid). Hydrogen atoms and perchlorate anions have been omitted for clarity.

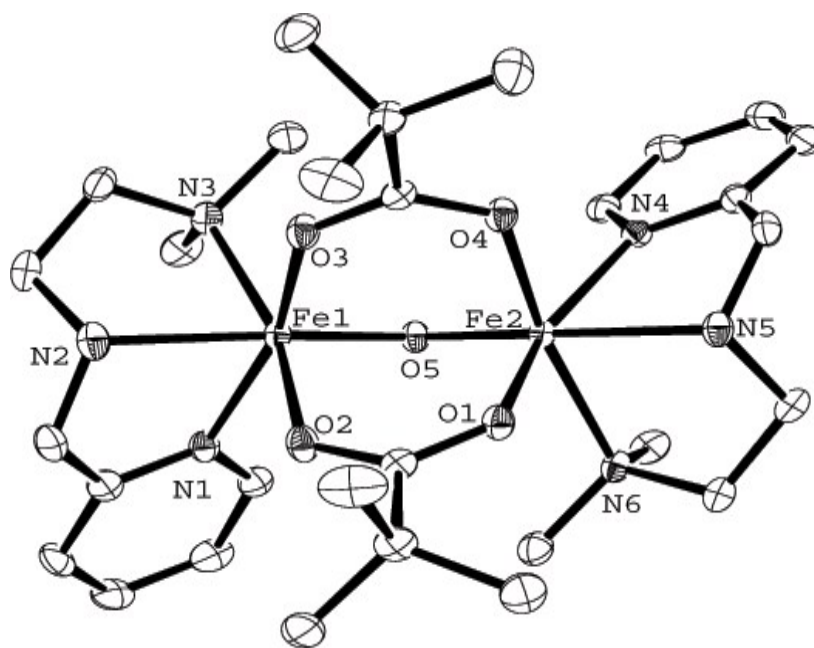


**Figure 2.** Molecular structure of  $[\text{Fe}_2\text{O}(\text{L})_2(\text{Me}_3\text{Ac})_2](\text{ClO}_4)_2$  **3** (40% probability factor for the thermal ellipsoid). Hydrogen atoms and perchlorate anions have been omitted for clarity.

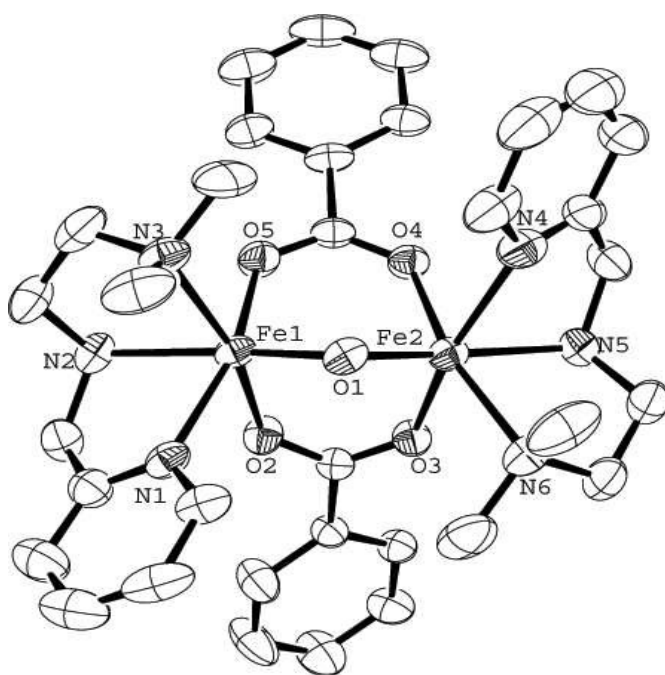


**Figure 3.** Molecular structure of  $[\text{Fe}_2\text{O}(\text{L})_2(\text{OBz})_2](\text{ClO}_4)_2$  **4** (40% probability factor for the thermal ellipsoid). Hydrogen atoms and perchlorate anions have been omitted for clarity.

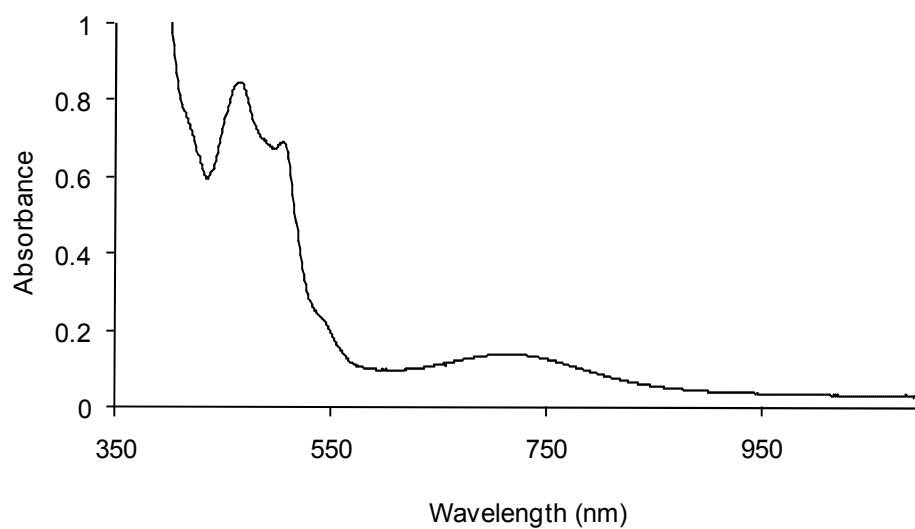


**Figure 4.** Electronic absorption spectra of  $[\text{Fe}_2\text{O}(\text{L})_2(\text{OAc})_2](\text{ClO}_4)_2$  ( $6 \times 10^{-4}$  M) in DCM:ACN mixture at 25 °C

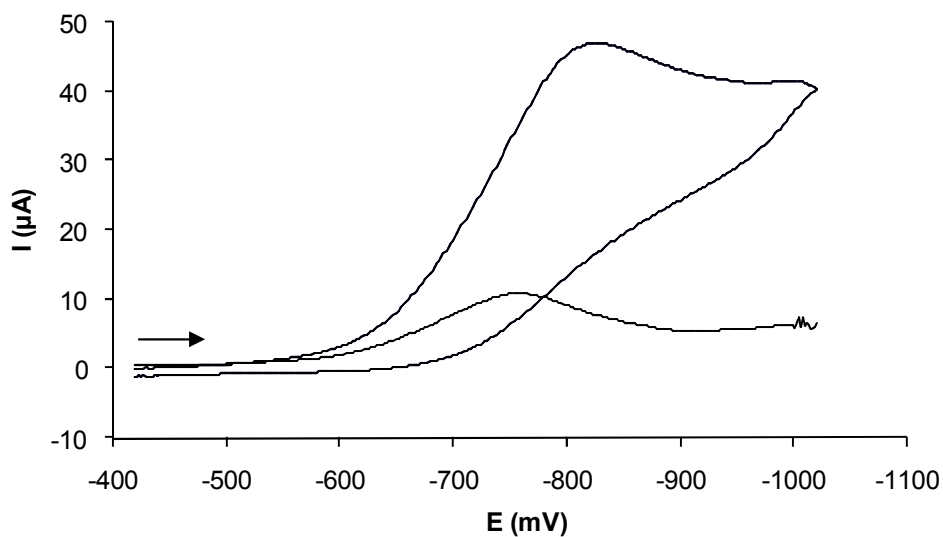


**Figure 5.** Cyclic voltammogram (CV) and differential pulse voltammogram (DPV) of 1 mM complex  $[\text{Fe}_2\text{O}(\text{L})_2(\text{OAc})_2](\text{ClO}_4)_2$  in a dichloromethane-acetonitrile solvent mixture at 25 °C. Supporting electrolyte: 0.1 M TBAP. Scan rate:  $50 \text{ mV s}^{-1}$  for CV and  $5 \text{ mV s}^{-1}$  for DPV.

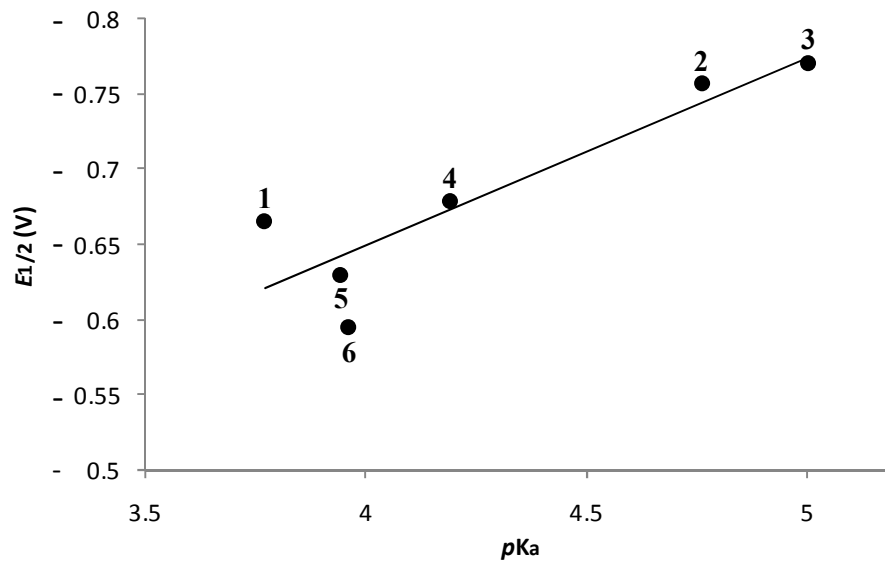


**Figure 6.** A linear correlation ( $R^2$ , 0.80) between  $pK_a$  value of bridging carboxylates and  $E_{1/2}$  value of diiron(III) complexes

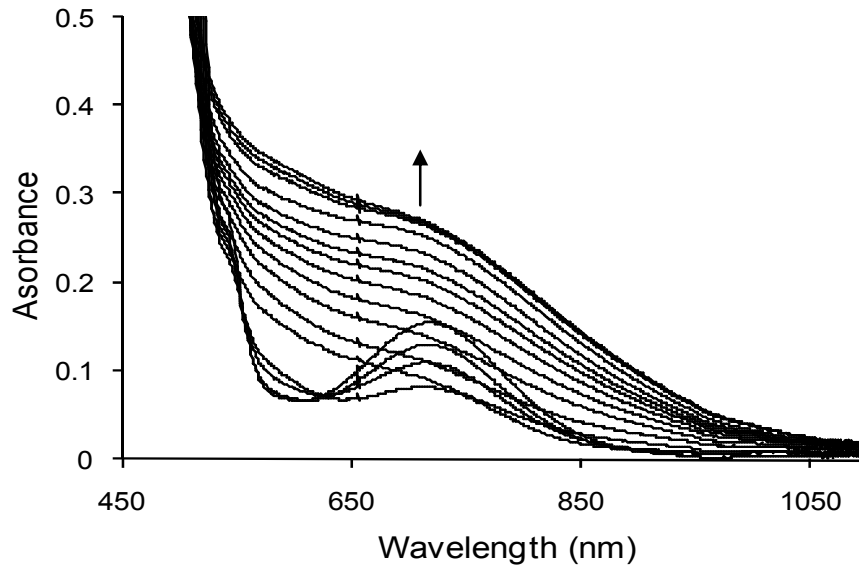


**Figure 7.** Reaction of complex **4** with *m*-CPBA (5 equiv.) and triethylamine (1 equiv.) followed by UV-Visible spectroscopy at room temperature.